TECHNICAL MEMORANDUM

678

Atmospheric Motion Vectors from model simulations. Part II: Interpretation as spatial and vertical averages of wind and role of clouds

A. Hernandez-Carrascal and N. Bormann

Research Department

October 2012

European Centre for Medium-Range Weather Forecasts
Europäisches Zentrum für mittelfristige Wettervorhersage
Centre européen pour les prévisions météorologiques à moyen terme

Series: ECMWF Technical Memoranda

A full list of ECMWF Publications can be found on our web site under:
http://www.ecmwf.int/publications/

Contact: library@ecmwf.int

European Centre for Medium-Range Weather Forecasts
Shinfield Park, Reading, RG2 9AX, England

Abstract

The main objective of the study described here is to improve the characterization of Atmospheric Motion Vectors (AMVs) and their errors to improve the use of AMVs in Numerical Weather Prediction (NWP). AMVs are estimates of atmospheric wind derived by tracking apparent motion across sequences of meteorological satellite images, and it is known that they tend to exhibit considerable systematic and random errors and geographically varying quality, as shown in comparisons against radiosonde or NWP data. However, there is a rather limited knowledge of the characteristics and origin of these errors: they can arise in the AMV derivation process, but they can also arise from the interpretation of AMVs as single-level point observations of wind. An important difficulty in the study of AMV errors is the scarcity of collocated observations of clouds and wind.

To overcome that difficulty, this study approaches the analysis of AMV errors using a simulation framework: geostationary imagery is generated from high resolution NWP model simulations, and AMVs are derived from sequences of simulated images. The NWP model provides a "ground truth" and a sophisticated description of the atmosphere on a high-resolution grid at frequent timesteps, which allows a detailed study of AMV errors, bypassing the usual difficulty of the scarcity of observations. Provided model simulations are realistic, the analysis of AMV errors in this setting can shed light on the nature of AMVs derived from observed imagery and their errors. The study is performed on the basis of Meteosat-8 image simulations from the Weather Research and Forecasting (WRF) regional model, run with a nominal horizontal resolution of 3 km. SEVIRI channels IR10.8 and WV6.2 are used for the derivation of AMVs, and only AMVs obtained from cloudy scenes are used.

The study is described in two companion papers. The second part of the study, described here, focusses on observation operator aspects, i.e. on alternative interpretations of what AMV represent best. The key results are: 1) there is evidence that high level AMVs are more representative of the wind at a level within the cloud, rather than the cloud top; 2) in addition, interpreting the AMVs as vertical averages of wind can give some benefits, but these are relatively small compared to interpreting the AMVs as single-level wind estimates for a suitably-chosen level within the cloud; and 3) low-level AMVs seem to be more representative of a wind average over the cloud layer than of the wind at the base or the top of the cloud.

1 Introduction

AMVs are estimates of atmospheric wind derived by tracking apparent motion across sequences of meteorological satellite images, and it is known that these wind estimates tend to exhibit considerable systematic and random errors and geographically varying quality, as shown in comparisons against radiosonde or NWP data (e.g., Cotton and Forsythe, 2010). Traditionally, AMVs are interpreted as single-level point estimates of wind, and it is assumed that high-level AMVs represent best the wind at the top of the cloud layer and that low-level AMVs represent best the wind at the base of the cloud (Hasler et al., 1979). It is generally accepted that an accurate estimate of the cloud top height is essential in order to assign a suitable height to high-level AMVs.

This is the second of a two-part paper summarising results from a study that uses a simulation framework to better characterise current Atmospheric Motion Vectors (AMVs). In this type of framework, a simulation from a high-resolution model provides the "true" atmosphere, from which sequences of satellite images are generated which are subsequently used to derive AMVs. In the first part (Hernandez-Carrascal et al., 2012), we introduced the simulation used in this study, analysed the realism of the resulting simulated images, and investigated the characteristics of the derived AMVs by comparing these to the "true" wind from the model simulation. For the latter, we employed the traditional approach of interpreting AMVs as single-level point observations. Our results showed that the characteristics of the simulated

AMVs are broadly in-line with those from real AMVs, even though some errors and biases appear larger in the simulated data. Error correlations were also estimated, providing indications of significant spatial as well as temporal and vertical error correlations.

It has often been suggested that the traditional interpretation of AMVs as single-level point estimates of wind might be one of the causes of AMV errors (e.g., Rao et al., 2002; Velden and Bedka, 2009). The reason becomes apparent if we consider the process of AMV derivation. In the operational derivation of AMVs from geostationary imagery, apparent motion of radiance or Brightness Temperature (BT) patterns is tracked across images by using region-matching methods. The interval between consecutive images is currently in the range of 15 to 30 minutes, the size of the tracer boxes used in the tracking step is typically around 24x24 pixels (i.e. at least 75x75 km for a nominal horizontal resolution at nadir of 3km), and radiances represent the contribution of a vertical layer, especially in the case of clear-sky areas in water vapour (WV) imagery. It has been suggested that considering what the images represent and how AMVs are derived, it would be more appropriate to interpret AMVs as vertical, horizontal and time-averaged estimates of wind (e.g Rao et al., 1990; Büche et al., 2006).

In order to test whether it is appropriate to interpret AMVs in a certain way, the model wind according to that interpretation is calculated, and then AMVs are compared against collocated model winds to produce the usual statistics. The process of calculating an observation equivalent from model fields is also referred to as the "observation operator" in data assimilation. A well designed observation operator and a good knowledge of the characteristics of the observation errors are needed in order to make an optimal use of that type of observation by the assimilation system.

A number of studies have investigated the effect of interpreting the AMVs as an average wind over a layer in the vertical, by comparing the AMVs against radiosonde data (e.g., Rao et al., 2002; Velden and Bedka, 2009) or short-term forecasts (e.g., Bormann et al., 2002; Forsythe et al., 2010). In these studies, the layer mean is calculated as a weighted average, using either top-hat or Gaussian weighting functions. The layers can be positioned around the originally assigned level, or with their center offset relative to the originally assigned level. Using an approach in which the layer was positioned below the originally assigned pressure for high level winds, Velden and Bedka (2009) found that the AMVs compared better to radiosondes when the radiosondes were averaged over layers of around 30-100 hPa for cloudy infrared or water vapour winds. As their study was based on AMVs collocated with three radiosonde sites only, the wider applicability of the results is unclear. Forsythe et al. (2010) also found some benefits from calculating AMV-equivalents from short-term forecasts as averages in the vertical, yet they argued that the depth of the layer may need to be situation-dependent to achieve the full benefit.

A high-resolution model simulation provides not only ground-truth winds, but also a very detailed description of the "true" atmosphere on a high-resolution grid. Cloud related variables, such as liquid-water mixing ratio or ice mixing ratio, are either part of the simulation output or can be calculated from it. The detailed description of the atmosphere allows the exploration of alternative interpretations of AMVs involving e.g. the vertical location of cloud layers, and also to study how specific conditions of the ambient cloud affect AMV quality. The simulation framework allows a more detailed and focussed analysis than is normally possible when using real observations.

In the current study, we use the possibilities open by the simulation framework to explore alternative interpretations of AMVs as vertical as well as spatial averages, and the impact of reassigning AMVs to vertical levels or layers related to the model ambient cloud layer. In particular, we revisit the traditional assumption that high-level and low-level AMVs best represent, respectively, the wind at the top and at the base of the ambient cloud layer.

The structure of the paper is as follows. Section 2 describes briefly the data used in the study. Section

3 focusses on the interpretation of AMVs as horizontal and vertical averages of wind. Section 4 concentrates on AMV observation operators that include cloud variables. Section 5 explores other aspects related to the role of clouds, and section 6 concludes the paper, summarizing and pointing at directions for future work.

2 Data

In this section, we give a short description of the simulation and datasets used in the study. The reader is referred to the companion paper (Hernandez-Carrascal et al., 2012) for details.

The model used for the simulation is the Weather Research and Forecasting (WRF) regional model, with a nominal horizontal resolution of 1.7-3 km. The simulated images replicate the geometry and resolution of Meteosat-8 SEVIRI images. The study period spans 24 hours, starting 16 August 2006, and the study area is the prime disk covered by MSG at 0° longitude within the latitudes 58°S / 58°N, restriction due to the model simulation.

The WRF is a compressible non-hydrostatic regional NWP model, described in Skamarock et al. (2005). The WRF includes various microphysical quantities as prognostic variables, parameterized using the Thompson et al. (2008) mixed-phase cloud microphysics scheme. This sophisticated microphysics scheme is a particularly important characteristic for this study. An existing simulation with the WRF model was used in this study, kindly provided to ECMWF by CIMSS and further described in Otkin et al. (2009). The dataset was produced with version 2.2 of the WRF, run over a domain covering the prime Meteosat disk (within 58° latitude), with a resolution that varies from 3 km at the equator to 1.7 km at the N and S boundaries, and 52 vertical levels (model top at 28 hPa). The WRF was initialised on 15 August 2006 18Z, from 1° analyses from the Global Data Assimilation System (GDAS). The study period is covered through a 6-30 h forecast, i.e. a six hours spin-up period was allowed for the simulation to develop fine scale structures from coarser initial conditions. The fields from the simulation output were available on timesteps of 15 min throughout the study period.

SEVIRI images from the WRF simulation output were produced every 15 min over the study period using version 9 of the RTTOV radiative transfer package (Saunders et al., 2008). All 8 infrared and near-infrared channels of SEVIRI were simulated over the study area. AMVs were derived by EUMETSAT from the WRF simulated imagery (SEVIRI channels IR10.8 and WV6.2), using a prototype derivation system developed in preparation for Meteosat Third Generation imagery (Borde et al., 2011). AMVs were produced half-hourly, from triplets of images. Only cloudy AMVs were produced for this study.

3 AMVs interpreted as vertical and horizontal averages of wind

This section concentrates on the evaluation of AMVs interpreted as wind averages. We consider calculating AMV-equivalents from the model data by averaging over layers in the vertical as well as over neighbourhoods in the horizontal. The approach for averaging in the vertical is similar to that used in Velden and Bedka (2009). It must be emphasized that all the AMVs in this study were derived from cloudy tracers. If tests similar to the ones presented here were applied to clear-sky AMVs, the results would presumably be quite different, as radiances in clear-sky tracers represent the contribution of deeper tropospheric layers.

3.1 Method

For each AMV in the study set, a set of relevant data were extracted from the stored model fields at the same time, to help with the calculations. Given the latitude and longitude of an AMV, for each model level from 1 (closest to surface) to 45 (around 80 hPa), the following values were obtained: u and v at the nearest gridpoint, and two neighbourhood averages of u and v, for radii of 30 km and 40 km. Therefore, three wind profiles associated to each AMV were available for subsequent calculations: 1) u and v at the nearest gridpoint, 2) u and v averaged on a 30-km radius neighbourhood, and 3) u and v averaged on a 40-km radius neighbourhood. Throughout the section, the labels used to identify these profile types are *NR0*, *NR30* and *NR40*, respectively.

Regarding vertical averages, two types of layer were considered:

centre : The layer is centred on the pressure originally assigned to the AMV: if *amv_pres* represents the original pressure of the AMV, and Δp the depth of the layer for the average, the pressure interval used for the average is $[p_0, p_1] = [amv\_pres - \Delta p/2, amv\_pres + \Delta p/2]$.

below : The layer is located just below the AMV level in the vertical, i.e. the pressure interval used for the average is $[p_0, p_1] = [amv\_pres, amv\_pres + \Delta p]$.

All vertical averages were calculated using a boxcar weighting function. In some cases, the pressure interval $[p_0, p_1]$ was not fully contained in the pressure interval determined by the first and last model levels in the considered profile; this happened particularly for low-level AMVs for deep layers, but also to some extent for high level AMVs. In those cases the averaging interval was reduced as needed.

When AMVs were interpreted as single-level point estimates of wind, for each AMV the model wind was obtained as linear interpolation of the collocated model profile (*NR0*) to the chosen pressure.

For comparisons, we also considered the case of interpreting the AMVs as single-level point estimates of wind, but with a systematic shift in the height assignment:

new_HA : The AMV is reassigned lower in the atmosphere by a pressure increment Δp to $amv\_pres + \Delta p$, and interpreted as single-level estimate of wind.

3.2 Results

In this section, the expression *height bias* is used often; with it we mean a bias with respect to the most representative level for AMVs, i.e. the level leading to the best overall statistics), not a bias with respect to the cloud top.

Figures 1 and 2 show how the comparison statistics vary with layer depth, for high level water vapour and infrared AMVs, respectively. When the model wind is calculated as an average over a layer centred on the original AMV pressure (*centre*), both the root mean square vector difference (RMSVD) curves (left panels) and the bias curves (right panels) show a consistent picture for the three latitude bands: an improvement as the layer depth increases, almost all the way from 0 to 300 hPa. When the model wind is calculated as an average over a layer placed just below the originally assigned level (*below*), the figures show a clear overall improvement with respect to the *centre* curves. For the three latitude bands, the RMSVD *below* curves show better values than those of the *centre* curves for depths up to around 220 or 240 hPa. The differences are particularly large for the tropics. Both the RMSVD and the bias curves

show an optimal depth in the region of 120-160 hPa for the water vapour winds, and 180-220 hPa for the infrared winds for the three latitude bands for this type of vertical averaging.

In the case where the averaging is performed over a layer below the assigned level, most of the improvement comes from implicitly increasing the assigned pressure of the AMVs. This can be seen by comparing the statistics for the *below* and *new_HA* curves in Figures 1 and 2. For the latter case, the AMV is simply reassigned lower in the vertical, to the centre of the layer used in the *below* case, but otherwise treated as single-level point observation. The similarity between the RMSVD and bias curves is very striking, particularly around the optimal Δp, and the improvement from layer averaging is comparatively small. The statistics suggest an optimal mean downward reassignment of around 60-80 hPa for the high level water vapour winds and 90-100 hPa for the high level infrared winds.

Mid and lower level AMVs show a similar behaviour: there is a clear improvement both in RMSVD and speed bias when the effective height of the AMVs is lowered, either by calculating model equivalents as averages over a layer below the originally assigned height or by reassigning the AMVs to a lower level (Figures 3 and 4). Most of this improvement comes from assigning the AMVs lower in the atmosphere rather than the layer averaging (compare *below* and *new_HA* curves). In contrast, averaging around the originally assigned level leads to little or no improvement, even for very large layer depths. For middle-levels, the statistics suggest a very large systematic error in the height assignment of the AMVs of 150 hPa or more, whereas for the low levels this bias is around 100 hPa.

We also investigated the effect of calculating the model equivalents as horizontal averages, and while this again leads to some benefits, the improvements are very small. Table 1 shows statistics for high-level WRF WV6.2 AMVs, evaluated as vertical averages over an interval of 140 hPa (layer position: *below*) and horizontal averages for different neighbourhood radii (*NR0*, *NR30* and *NR40*). The reason for choosing 140 hPa for the depth of the layer is that this is approximately the optimal depth, according to Figure 1, and therefore it is where the effect of the horizontal averaging can be appreciated better. For the three latitude bands, the RMSVD is slightly better for *NR30* than for *NR0*, and very similar for *NR30* and *NR40*; a similar pattern can be noticed for other depths (not shown). Regarding the speed bias, it is also better for *NR30* than for *NR0*, and very similar for *NR30* and *NR40*; however, this is not a consistent pattern, and the opposite is true for other depths (not shown).

Meteosat-8 WV6.2 AMVs - High level, QI > 80%, layer: [0, 140], layer pos: below									
	NH			**TR**			**SH**		
	NR0	**NR30**	**NR40**	**NR0**	**NR30**	**NR40**	**NR0**	**NR30**	**NR40**
Number	16499	16499	16499	36289	36289	36289	39205	39205	39205
Speed bias [m/s]	0.154	0.134	0.119	0.947	0.882	0.856	0.488	0.462	0.445
AMV speed [m/s]	21.25	21.25	21.25	13.80	13.80	13.80	37.81	37.81	37.81
RMSVD [m/s]	6.74	6.67	6.66	5.99	5.87	5.87	7.96	7.89	7.87
NRMSVD [m/s]	0.317	0.314	0.313	0.434	0.425	0.425	0.210	0.209	0.208

Table 1: Summary statistics for high-level AMVs derived from WRF simulated WV6.2 images, evaluated as horizontal and vertical averages. Only winds with a model-independent QI > 80% have been used.

It should be noticed that no attempt was made to separate results according to the local horizontal variation of wind. That the differences between different neighbourhood radii are so small could be a consequence of the wind being a smooth field for high levels (with notorious exceptions such as the jet). Restricting the analysis to cases of significant horizontal variation would likely give a better insight into

the value of horizontal averaging in specific cases. It should also be noted that the effective resolution of the model wind field will be lower than the nominal grid resolution (1.7-3 km), and the inherent smooth representation means that the effect of spatial averaging of the wind field may be underestimated in our simulation framework. This also holds for the vertical representation which is subject to the model's effective vertical resolution.

3.3 Discussion

The results of this study, regarding vertical averaging, are to a large extent consistent with the findings of previous studies involving the comparison of AMVs with vertical averages of wind (Velden and Bedka, 2009; Forsythe et al., 2010). Velden and Bedka (2009) compared AMVs from NOAA/NESDIS operations with radiosonde observations of winds at three different locations, and they found a consistent better agreement between AMVs and layer-averaged radiosonde wind than between AMVs and the radiosonde wind at the assigned AMV pressure, with optimal depths varying between 30 and 100 hPa for cloudy AMVs, depending on radiosonde site, height assignment method, vertical level and spectral band. Forsythe et al. (2010) compared real AMVs from Meteosat-9 IR10.8 imagery with first-guess observation equivalents in the Met Office system, treating AMVs as layer observations, and found a small reduction in mean vector difference (MVD) when AMVs were interpreted as vertical averages, compared to the traditional interpretation. However, they found that the best results were obtained for layers of 20-60 hPa depth. The difference concerning the optimal layer depth might be due, at least partly, to different height biases, although other factors could be at play.

The results shown so far suggest that the height assignment used in the current study has an overall tendency to place the AMVs too high in the vertical, with a bias of around 80-100 hPa. This bias is meant as a bias with respect to the most representative level for AMVs, i.e. the level leading to the best overall agreement between AMVs and the truth), not a bias with respect to the cloud top. Comparisons between best-fit pressures and the originally assigned pressure also point to a bias of such magnitude (not shown). This height bias appears to be present in the tropics as well as the extra-tropics, and at all levels. The bias appears very large, and it is also larger than indications of height assignment biases obtained with real AMVs in the past. These are typically of the order of a few tens of hPa (e.g Salonen et al., 2012; Bormann et al., 2002).

A number of factors may contribute to such a large height bias. It is possible that part of it is the result of small differences in the bias characteristics of the observed and simulated brightness temperatures, leading to a bias in the height assignment to the cloud top that is specific to the current simulation. The realism of semi-transparent clouds will be particularly important for the high level winds, and systematic short-comings either in the WRF simulation or the radiative transfer may also contribute to the biases seen here. The bias may also be partly due to a bias in the CLA (cloud analysis) product used to estimate the height of cloud tops in the AMV derivation prototype, or to the use of the CCC method (and the threshold applied) to identify the feature tracked, as this determines the pixels that are taken into account in the final estimate of the AMV height. Finally, the benefit of assigning the AMVs to lower heights may support the hypothesis that the cloud top is not the most representative height for AMVs, and instead a lower height or layer would be more appropriate. This aspect will be investigated further below.

3.4 Conclusions

The main findings from the experimentation with the simulated AMVs described in this section are:

- Horizontal and vertical averaging of model wind consistently leads to better agreement between the AMVs and model equivalents, but the improvement brought by vertical averaging is generally small, and the improvement brought by horizontal averaging is very small.
- Reassigning AMVs to lower heights in the vertical brings a considerable improvement regarding both RMSVD and bias. Overall, the optimal pressure increment is around 60 to 80 hPa for high-level AMVs derived from the WRF WV6.2 simulated imagery, and around 90 hPa for the IR10.8 imagery. An interesting point to notice is that the optimal pressure increment is roughly the same for both RMSVD and bias.

When biases in the AMV height assignment are large, the improvement brought by implicitly reassigning AMVs to a different level masks the benefits of averaging, and therefore make it difficult to accurately assess the improvements yielded by interpreting AMVs as averages. Even in the case of smaller height biases, it is not trivial to separate the issues of layer depth and height assignment errors, as already pointed out by Forsythe et al. (2010).

We would like to emphasise that these results originate from a specific model simulation and a specific AMV derivation system. While the results regarding the improvements brought by averaging are likely to be similar for other simulations or derivation systems, as they relate to the nature of AMVs, the results regarding the improvements brought by reassigning AMVs to higher pressures will be very dependent on the specific AMV derivation system used in the study, and in particular to the height assignment algorithm, and to some extent also to the model simulation.

Another point we would like to stress is that all the AMVs in the dataset were obtained by tracking cloudy tracers. Considering the nature of WV imagery, it is not likely that the tests described in this section would yield similar results if they were applied to clear-sky AMVs.

4 Observation operators that involve cloud variables

In this section we explore observation operators that take into account the location and characteristics of cloud layers. This is only possible thanks to the detailed description of the atmosphere that a high-resolution model simulation provides. This model information is used in two ways: firstly, to identify atmospheric situations for which the interpretation of AMVs should be simpler, and secondly, to aid the interpretation of the AMVs themselves, for instance by attributing the AMVs to heights or layers obtained from the distribution of the model clouds directly.

4.1 Methods

4.1.1 Classification of AMVs according to collocated model cloud profiles

A simulation framework allows to design model-based classifications of ambient cloud profiles. In this study we use a simple classification of AMVs, according to the characteristics of collocated model profiles, into ice/liquid and single/multi-layer cloud situations. The main purpose of this classification is to identify multilayer situations and to distinguish between ice and liquid-water cloud layers, and it has the advantage that it is based directly on model output.

A more sophisticated classification that also distinguishes, for instance, convective and non-convective cases would be possible but is beyond the scope of the current study. Alternatively, cloud classifications

into cloud types designed for observed images could be adopted for simulated imagery; such a classification would be more sophisticated, but on the other hand it would introduce intermediate products between the model output and the classification, and therefore possibly errors.

We classify the cloud profiles into the four categories shown in Table 2. The classification considers the profiles of cloud fraction and the total mixing ratios of all liquid or ice species of the WRF model combined. These were obtained from a neighbourhood with a radius of 30 km around the assigned AMV location, with the cloud fraction being the relative frequency of cloudy grid points in the neighbourhood, and the mixing ratios calculated as the average over the cloudy grid points. Ideally, this step should have taken into account the extent of the actual feature tracked in the AMV derivation (in this study through the CCC method - e.g. Borde and Oyama, 2008). However, this information was not available in the AMV dataset, and instead a neighbourhood consistent with the typical feature size was used. Note that simply using the WRF cloud information from the gridpoint nearest to the AMV location was found inappropriate in this context, due to the large spatial variability of clouds. For our classification, a model level is considered cloudy if more than 15 % of the model grid points in the 30 km neighbourhood are cloudy, and the mean ice mixing ratio (respectively liquid-water mixing ratio) is above a threshold value of 10^{-4} g / kg. An ice (respectively liquid-water) cloud layer is formed by a set of consecutive ice (respectively liquid-water) cloud levels. In the classification of AMVs from WV6.2 imagery, cloud levels below 700 hPa were ignored, as their contribution to the top-of-atmosphere radiance is negligible for this channel.

Label	**Description**
Clear	No cloud layers present in the model profile
Ice1	One ice cloud layer (and no liquid-water cloud layers)
Liq1	One liquid-water cloud layer (and no ice cloud layers)
Multilayer	Several liquid or ice cloud layers

Table 2: Cloud profile types according to the number of ice cloud layers and liquid-water cloud layers.

Figure 5 shows an example of collocated profiles of several model variables for one particular AMV. In this example, there is one ice-cloud layer and one liquid-water cloud layer, and the profile would be classified as *Multilayer*. This figure illustrates the kind of information that the model output can provide.

Table 3 shows the relative frequency of each cloud profile type, for AMVs derived from the WRF WV6.2 and WRF IR10.8 sets of simulated images. Two points are apparent: one is the high frequency of AMVs classified as clear according to the model profiles, especially in the case of WV6.2 imagery. This is surprising, considering that only cloudy tracers were used in the derivation process. This is partly the result of a short-coming of the cloud classification used in the AMV derivation. The cloud classification in the AMV derivation also considers low-level clouds, even though these are unlikely to be visible in the water vapour channel. In addition, small differences in the biases in the simulated dataset may also lead to mis-classifications during the AMV derivation.

Another striking point is the high occurrence of multilayer situations. It is generally recognized that multilayer situations are very challenging and not handled well by current operational derivation systems, both in terms of the tracking and the height assignment; the high occurrence implies that it is potentially an important source of AMV errors. However, it should be noticed that this classification has a tendency to overestimate the occurrence of multilayer situations. In some scenes that are multilayer from the model

perspective, the contribution from lower layers to the top-of-the-atmosphere radiance is negligible, i.e. the image may only represent cloud information from the top layer. In addition, cases such as one mixed ice and liquid-water cloud layer would be labelled as multilayer according to this classification. The main purpose of the classification is to identify situations for which height assignment should be less problematic.

	WRF IR10.8 AMVs	WRF WV6.2 AMVs
Clear	6.4	29.9
Ice1	11.7	43.6
Liq1	29.9	2.2
Multilayer	52.0	24.3

Table 3: Relative frequency [%] of each cloud profile type for the dataset of AMVs derived from the WRF IR10.8 and WV6.2 sets of simulated images.

4.1.2 Model wind calculations

In the following, we consider different interpretations of AMVs (or observation operators) and make use of the cloud information provided from the model data to attribute the AMV to a certain level or layer. The cloud layer definition is the same as in the previous sections, and the cloud top/base are the highest/lowest model level considered cloudy. When AMVs are interpreted as single-level point estimates of wind, the model wind is calculated by linear interpolation of the nearest-gridpoint wind profile to the chosen pressure. The following interpretations are used:

pTop : AMVs interpreted as single-level point estimates of wind at the top of the model cloud. Note that this is the traditional view of what high-level AMVs best represent.

pBot : AMVs interpreted as single-level point estimates of wind at the bottom of the model cloud. Note that this is the traditional view of what low-level AMVs best represent (following Hasler et al., 1979).

pMean : AMVs interpreted as single-level point estimates of wind, at a pressure within the model cloud. This pressure is calculated as an average over the top cloud layer, with weights proportional to the ice (or liquid-water) mixing ratio; it tends to be close to the maximum of the liquid or ice water mixing ratio.

VerAve : AMVs interpreted as an average of wind over the top model cloud layer. In this case, the model wind is calculated as an average, over all the model levels from the bottom to the top of the layer, of the neighbourhood-averaged profiles of u and v.

For reference, two further model winds are calculated:

LinInt : The usual interpretation of AMVs as single-level point estimate of wind at the pressure assigned to the AMV during the derivation.

LBF : The model wind at the level of best fit (LBF) pressure, defined as the pressure minimizing the vector difference between (u,v) from the AMV and (u,v) from the model nearest-gridpoint wind profile, assuming a linear variation of u and v between model levels.

4.2 Results

In the following, we restrict our analysis to cases with a single cloud layer, as this simplifies the investigations into a relationship between the model cloud and the derived wind. For these cases, there is no ambiguity regarding the cloud layer used for the alternative ways of calculating model winds, and also the difficulties brought by multilayer situations are avoided.

4.2.1 High-level AMVs

Figure 6 shows 2D histograms of speed for high-level AMVs derived from the WRF WV6.2 simulated imagery, for northern hemisphere extra-tropics with a model-independent $QI > 80\%$. The selection is restricted to scenes with exactly one ice cloud layer (*Ice1*). The figure shows histograms for four types of model-equivalent winds: *LinInt*, *pTop*, *pMean* and *VerAve* (see section 4.1 for a detailed description of each label). Figures 7 and 8 show similar histograms, for tropics and southern hemisphere extra-tropics, respectively. Table 4 shows summary statistics for the same AMVs and model-equivalent winds.

WRF WV6.2 AMVs - High lev, QI > 80%, Ice1				
		NH	**TR**	**SH**
Number		11796	22745	25190
AMV speed [m/s]		21.65	14.46	36.49
Speed bias [m/s]	**LinInt**	-1.903	0.556	-3.464
	pTop	-3.186	-2.282	-4.042
	pMean	-0.169	0.678	3.350
	VerAve	1.095	2.028	4.488
RMSVD [m/s]	**LinInt**	8.40	12.13	10.59
	pTop	8.87	9.61	11.85
	pMean	6.65	5.05	10.57
	VerAve	6.76	5.74	10.37

Table 4: Statistics for high-level AMVs with exactly one ice cloud layer, from WRF WV6.2 images, for different ways of calculating the model wind.

Figures 6 to 8 and Table 4 show that calculating the model wind by linear interpolation of the model wind profile to the pressure assigned to the AMV (*LinInt* label) leads to a considerable slow bias in the extra-tropics, and to a fast bias and a very large dispersion in the tropical region. Assigning each AMV to the top of the cloud layer (label *pTop*) leads to very marked slow biases (including the tropics), while the overall appearance of speed histograms looks quite similar to those of *LinInt*. Reassigning each AMV to a pressure in the middle of the cloud (label *pMean*) leads to a clear improvement regarding bias and RMSVD in the northern hemisphere and to a much better RMSVD in the tropics; over the southern hemisphere, the agreement between AMV and model speed is also improved (Figure 8), even though the

RMSVD and speed bias shown in table 4 do not reflect this, due to the presence of a number of outliers. Calculating the model wind as an average over the cloud layer (label *VerAve*) leads to a fast bias in all the latitude bands, particularly marked for the southern hemisphere, and overall similar values for RMSVD as with the *pMean* calculation. Overall, interpreting the AMVs as representing wind at a level within the model cloud produces the best results.

One possible explanation for the outliers in Figure 8 is that when the cloud layer is very deep, the *pMean* tends to produce a too high pressure, i.e. to locate AMVs too low in the vertical, towards levels that are already totally obscured by the cloud in the imagery. To test this explanation, similar statistics were produced for a variant of *pMean*. In this variant, the model wind was obtained by linear interpolation of the nearest-gridpoint wind profile to the pressure $pMCap = max(pMean, pTop + cap)$, for $cap = 100\ hPa$. The choice of *cap* took into account the results shown earlier in the paper, but it was somewhat arbitrary, and the best choice is likely to depend on the cloud optical depth. Figure 9 and Table 5 show, respectively, the 2D speed histograms and the RMSVD and bias values obtained when using *pMCap* for WRF WV6.2 AMVs for southern hemisphere extra-tropics. A comparison with Fig. 8 shows that the amount of outliers decreases considerably, and a comparison with Table 4 shows that there is a clear improvement in RMSVD and bias when AMVs are assigned to the *pMCap*.

WRF WV6.2 AMVs - High lev, SH QI > 80%, Ice1, pMCap	
	SH
Number	25190
AMV speed [m/s]	36.49
Speed bias [m/s]	0.061
RMSVD [m/s]	7.59

Table 5: Statistics for southern hemisphere extra-tropics, high-level AMVs with exactly one ice cloud layer, from WRF WV6.2 images, for pMCap model wind.

To further highlight the relationship between the model cloud top, the originally assigned pressure level, and the level of best fit, Figure 10 shows histograms of differences between these alternative pressure levels. The left column of Figure 10 shows histograms of the difference $pTop - pAMV$ between the pressure of the model cloud top and the originally assigned pressure, for high-level WRF WV6.2 AMVs, for the *Ice1* subset, for the three latitude bands. The histograms show that the pressure assigned during the derivation tends to be lower than the model cloud top for tropics, i.e. AMVs tend to be placed too high in the vertical with respect to the model cloud top, while the opposite is the case for the extra-tropics. For the subset studied, the AMV height assignment algorithm does not seem to have a clear overall tendency to underestimate or overestimate the pressure of the cloud top. The histograms are consistent with the finding that assigning the AMVs to the originally assigned pressure or to the model cloud top gives broadly similar results for the extra-tropics (see top panels of Figures 6 and 8 and the RMSVD values in Table 4).

The right column of Figure 10 shows histograms of the difference $pTop - pLBF$ between the pressure of the model cloud top and the best fit pressure, for the same AMVs dataset as in the left column of the figure. Notice that the AMV height assignment does not play any role here, as both *pTop* and *pLBF* pressures are model values.

The three panels show that, for the subset tested, the *pLBF* is clearly larger than *pTop*, that is the best

fit level tends to be below the cloud top in the vertical, typically by around 50 hPa. These results are consistent with the earlier finding that a height assignment lower in the atmosphere leads to better results (e.g., Figure 1 and Figures 6 to 8), and give further evidence to support the hypothesis that the best pressure to assign AMVs is not that of the cloud top, but a pressure within the cloud.

The two columns of Figure 10 link the two aspects of AMV height assignment: 1) What is the most appropriate level for the assignment of AMVs?, and 2) How to estimate that level in height assignment algorithms? A simulation framework provides the true wind profile, on the one hand, and a detailed description of cloud layers, on the other, and therefore allows to study separately how good the estimation of the cloud top pressure is in a particular AMV dataset, and whether the cloud pressure top is the most representative level for AMVs.

The results shown in this section suggest that assigning high-level AMVs to a representative level within the cloud layer (*pMean* or *pMCap*) significantly improves the agreement between AMVs and the model truth equivalent. Most importantly, speed biases are close to zero for this choice of height assignment. The results also suggest that assigning AMVs to an estimate of the cloud top for high level AMVs will introduce a bias, and instead a lower height that depends on the structure of the cloud is required. This aspect may have important implications for the use of cloud top pressure products for AMVs: a product that more accurately determines the cloud top may give rise to poorer speed biases for AMVs compared to a product that has been tuned for AMV requirements, as the AMV product will have been tuned to assign the AMVs lower within the cloud. Corrections to such accurate cloud top products may be needed to get the best benefit for AMVs.

4.2.2 Low-level AMVs

We will now consider low level AMVs. To simplify the interpretation, we again restrict the sample of winds to scenes with exactly one liquid-water cloud layer (*Liq1*). Figure 11 shows 2D histograms of speed for low-level AMVs derived from the WRF IR10.8 simulated imagery, for northern hemisphere extra-tropics with a model-independent $QI > 80\%$. The figure shows histograms for four types of model-equivalent winds: *LinInt*, *pBot*, *pMean* and *VerAve*. Figures 12 and 13 show similar histograms, for tropics and southern hemisphere extra-tropics, respectively. Table 6 shows summary statistics for the same AMVs and model-equivalent winds, and it also includes RMSVD and bias for *pTop*.

Comparing the results for the different interpretations of AMVs, there is a clear improvement when the model-equivalents for low-level AMVs are calculated with any kind of knowledge of the location of the model clouds. Reassigning each AMV to the bottom (*pBot*), the top (*pTop*), or a level within the cloud (*pMean*), as calculated from the model cloud data, leads to better statistics than when the originally assigned pressure level is used (*LinInt*). This suggests that the AMV derivation algorithm appears to struggle to estimate a pressure level that is appropriate for low level clouds. Interpreting the AMVs as an average wind over the cloud layer (*VerAve*) gives the best results in terms of the RMSVD, with a clear advantage over the other model-equivalents considered, including the *pMean*.

There is no evidence from our statistics that low level AMVs best represent the wind at the cloud base. Assigning the AMVs to the base of the cloud (*pBot*) or the top (*pTop*) gives similar results in terms of speed bias and RMSVD (e.g., Table 6), whereas assigning the wind to a level within the cloud (*pMean*) leads to overall the best comparisons for single level interpretations of AMVs. Traditionally, low level AMVs are considered to best represent wind at the cloud base, following work by Hasler et al. (1979) and other considerations, but our statistics do not show evidence for this. Instead, it appears that an average over the cloud layer may be more appropriate.

WRF IR10.8 AMVs - Low lev, QI > 80%, Liq1				
		NH	TR	SH
Number		5440	50767	20813
AMV speed [m/s]		8.36	9.013	8.137
Speed bias [m/s]	**LinInt**	-0.317	1.639	0.4122
	pBot	-0.212	-0.449	-0.094
	pTop	-0.101	0.140	-0.063
	pMean	-0.153	-0.481	-0.212
	VerAve	-0.078	-0.315	-0.075
RMSVD [m/s]	**LinInt**	3.693	5.196	4.554
	pBot	2.971	2.947	2.802
	pTop	2.945	3.178	3.054
	pMean	2.651	2.711	2.609
	VerAve	2.341	2.326	2.186

Table 6: Statistics for low-level AMVs with exactly one liquid-water cloud layer, from WRF IR10.8 images, for different ways of calculating the model wind (see main text for a detailed description).

4.3 Conclusions

This section has shown how the detailed information on clouds provided by the model simulation output can be used to explore alternative interpretations of the nature of AMVs. As a first step, a basic classification of AMVs, according to the characteristics of collocated model profiles was presented. This classification allowed to restrict tests to specific cloud profiles in a very straightforward way.

We have explored a number of AMV observation operators, i.e. ways of calculating the model wind, involving cloud variables: 1) as single-layer point estimate of wind, reassigned to a cloud-average pressure, 2) as an average of wind over the cloud layer. We have also explored the reassignment of high-level AMVs to the pressure of the cloud top, and the reassignment of low-level AMVs to the pressure of the cloud base, as currently it is commonly accepted that these are the levels that AMVs represent best. The main conclusions are:

- Regarding high-level AMVs, reassigning AMVs to a cloud-average pressure leads to clear improvements, provided the cloud layer is not too deep. For deep clouds, it appears beneficial to restrict the cloud-average pressure to the upper part of the cloud.

- Regarding low-level AMVs from the WRF IR10.8 imagery, calculating the model wind as an average over the cloud layer gives the best results, regarding both RMSVD and bias. Interpolation to the bottom of the cloud fares worse, although it is still better than interpolation to the pressure assigned during the derivation, which suggests that the cloud pressure is not well estimated by the derivation algorithm.

5 Cloud characteristics and AMV quality

The detailed description of the atmosphere provided by the output of a simulation based on a high-resolution model able to resolve clouds explicitly allows to study how different ambient conditions affect AMV quality. In the following we will have a closer look at multilayer scenes and study the dependence of comparison statistics on the depth of the cloud layer.

5.1 Multilayer scenes

The classification of cloud profile types shown in Table 2 shows that multilayer scenes are very frequent. On the other hand, it is generally recognized that often they are not handled well by current operational AMV derivation algorithms if the top layer is semitransparent. This is therefore an area where progress could lead to an improvement in overall AMV quality, and also where a simulation framework could be of considerable help, as the model output provides details about cloud layer locations, ice and liquid-water mixing ratio, etc.

Figure 14 shows 2D histograms of wind speed for WRF IR10.8 AMVs for all cloud profile types ($CPT = ALL$), and for only one layer of ice-cloud ($CPT = Ice1$), for two model-equivalent winds (*LinInt* and *pMean*). The left panels show an area where AMV speed (around 10-15 m/s) is considerably lower than that of the model wind. This area does not appear in the right panels, which suggests that that problem is linked to multilayer situations. Two types of model wind have been included in the figure, to eliminate problems linked to a specific way of calculating the model wind. Notice that only AMVs with $QI > 80\%$ have been taken into account. The four histograms suggest an incorrect height assignment, related to multilayer situations, and resolved in a similar way for neighbour AMVs (as otherwise they would not have reached the QI threshold).

Figure 15 (top) shows an example of an interesting multilayer scene, which might offer an explanation for the problem described above. The two profiles on the left show that the wind has been assigned quite high in the troposphere, and that the best-fit pressure (marked as a horizontal line in the panel) is well defined and located lower in the vertical. The two profiles on the right show that the best-fit pressure coincides with a liquid-water cloud layer. A possible explanation is that a semitransparent ice-cloud layer allows patterns in the low liquid-cloud layer to be seen through, and the tracking algorithm captures the low level pattern while the wind is assigned to the high-level layer. The model-independent QI assigned to the AMV is 83%. Visual inspection suggest that this kind of situation is not frequent, but not uncommon. In similar cases, visualisation of the profiles of neighbour AMVs shows that the same type of pattern is often resolved in the same way, which explains the high QI assigned.

The lower panels of Figure 15 show a similar set of profiles for a multilayer scene which the AMV derivation resolved well. Visual inspection of these types of profiles shows that many multilayer scenes are well resolved, either because the cover and depth of the upper layer are such that the layer is sufficiently opaque (i.e. the contribution from the lower layers to the top-of-the-atmosphere radiance is negligible), or because the CCC method is successful in identifying the pattern tracked. Finally, there are also cases which are not well resolved, but that are marked with a low QI. The example shown in the upper panel of Figure 15 is therefore a worst-case scenario, which unfortunately seems to be not exceptional.

Figures 14 and 15 illustrate how the information provided by the model output can be used to study specific situations, e.g. multilayer situations. A simulation framework can bring new insight into multilayer scenes, and therefore help either to resolve them in a better way, or at least to detect them and flag them. Neighbour scenes tend to be resolved in the same way, and a QI based on internal consistency might

not be able to detect situations like the one described in Figure 15; therefore, marking multilayer scenes explicitly and including information about the global LBF would likely be of help to AMV users.

5.2 Impact of the depth of the top cloud layer

The purpose of the tests described in this section is to assess the impact of the depth of ice clouds on AMV quality. The motivation is that von Bremen (2008), in his study on AMVs derived from simulated imagery, hypothesised that thicker cirrus clouds represent more stable tracers, and therefore lead to AMVs that better represent the ambient wind. He found that, for cirrus clouds in environments with a small variation of wind speed with height, the AMV statistics improved with the vertical extent of the top cloud layer, although the number of AMVs in his test was very small.

Figure 16 shows average RMSVD and bias curves for varying depths of the top cloud layer, for all high-level AMVs from class *Ice1* (i.e. exactly one ice cloud layer), with a model-independent $QI > 80\%$ and a satellite zenith angle not larger than 70°, from WRF WV6.2 images (top) and WRF IR10.8 images (bottom). The depth of the layer has been calculated as the difference between the pressures of the cloud top and the cloud base; the AMVs were binned in intervals of 20 hPa, with the first interval $[0,20]$ including AMVs where the layer consists of one level, and the last interval including all AMVs for which the top layer has a depth above 500 hPa. Each panel shows the number of AMVs in each bin, and two pairs of RMSVD and bias curves, one for the model wind at the LBF (as a reference) and one for the model wind calculated as linear interpolation of a collocated model profile of wind to a layer-average pressure (label *pMean*; details described in section 4.1). The reason for selecting this way of calculating the model wind is that it was the one that showed best overall results in the comparison presented earlier in this section. The LBF-RMSVD curves serve as a lower bound, as by definition the LBF represents the best possible RMSVD value.

The statistics shown in Figure 16 do not support the hypothesis that AMVs derived from thicker ice cloud layers represent better the ambient wind than from thinner layers. While a slight decrease in RMSVD and bias with cloud depth can be seen in comparisons between AMVs and model winds at *pMean* in Figure 16 for very thin clouds, the sample size is very small, and the statistics are not considered representative. Moreover, the decrease does not appear in the curves for the LBF. For both IR10.8 and WV6.2 AMVs there is instead an increase in the RMSVD and speed bias from around 180 hPa, which is probably due to the nature of this model wind calculation (the average pressure over a deep layer is likely to underestimate the AMV's height). Furthermore, the RMSVD curve for the LBF is remarkably stable, if we leave bins with very few data aside; this supports the view that the progressive increase in RMSVD-*pMean* from around 180 hPa onwards is due to the model wind calculation method and not to the increased depth.

Figure 17 gives a more detailed picture for the WV6.2 set of AMVs; each panel shows results for one latitude band. Regarding the distribution of depths, perhaps the most noticeable point is that large depths are more frequent in the southern hemisphere extra-tropics than in the tropics or the northern hemisphere. Regarding RMSVD curves, the LBF curve appears quite stable for the three latitude bands; the curve for *pMean* shows an increase in RMSVD as depth increases, from around 180 hPa. The deterioration is particularly noticeable for the southern hemisphere extra-tropics, where deep layers are frequent. This is consistent with the earlier finding that assigning the winds to a "capped" version of the cloud-average wind (*pMCap*) provides a better level for the southern hemisphere winds.

It is worth noting that our results cannot be directly compared to von Bremen (2008). Von Bremen used an average model cloud layer wind in his comparisons, whereas we used assignment to a layer-average pressure and assignment to the LBF. Also he further restricted the sample of AMVs to situations with

little wind shear, and he used the number of model levels as a measure of layer depth. Moreover, the QI filters used in the two studies are also different. Nevertheless, our findings do not support his findings, and the reasons for this are unclear.

The test described here, regarding the impact of layer depth on AMV quality for ice clouds, is an example of how a simulation framework can help to study the impact on AMV quality of specific ambient characteristics.

6 Conclusions

The main objective of the study described in this paper has been to improve the understanding of the characteristics and origins of AMV errors, to improve the use of AMVs in Numerical Weather Prediction, and it has approached the analysis of AMV errors using a simulation framework. High-resolution model simulations provide a very sophisticated description of the atmosphere, including cloud variables, which has allowed to explore alternative interpretations of the nature of AMVs, and to study the impact on AMV quality of specific ambient characteristics.

First, we have presented evaluations of cloudy AMVs from WRF WV6.2 and IR10.8 simulated images, interpreted as horizontal and vertical averages. The main conclusions are:

- Horizontal and vertical averaging of model wind consistently leads to better agreement between the AMVs and model-equivalent winds, but the improvement is quite small.
- Reassigning AMVs to lower heights in the vertical brings a considerable overall improvement for high and middle level AMVs, regarding both RMSVD and bias, for the specific model simulation and AMV derivation prototype used.

Secondly, alternative interpretations of AMVs, related to the ambient cloud layer, have been evaluated. The main findings are:

- For high-level AMVs and ice clouds, AMVs are more representative of the wind at a level within the tracked cloud, rather than the cloud top.
- For low-level AMVs and liquid-water clouds, the AMVs are more representative of a wind average over the layer than of the wind at the cloud base or the cloud top.

Finally, we have shown how the detailed information on clouds provided by the model simulation output can be used to study how specific atmospheric situations affect AMV quality. Multilayer scenes are quite frequent according to this classification, and sometimes they are not handled well by current derivation systems. Detecting them and marking them as part of the quality information associated to AMVs could therefore help to make a better use of AMVs; information about the best fit pressure could be useful in this respect. We have also analysed the impact of the depth of ice cloud layers on high-level AMV quality; the tests carried out do not show any significant variation in RMSVD or bias when AMVs are reassigned to the LBF pressure, and therefore no impact on quality of the vertical extent of the ice cloud layer.

Our analysis has highlighted that one of the largest shortcomings in the current simulated WRF AMV dataset appears to be the height assignment which consistently underestimates the representative pressure. Several factors contribute to this: it is likely that the underestimation is partly due to mismatches

in bias characteristics between channels in the simulated and the observed imagery, possibly due to shortcomings in the radiative transfer model or upper level biases in the humidity or cloud fields in the WRF fields, and therefore specific to this simulation study. These could particularly affect the realism of the optical thickness of some cirrus clouds in the WRF simulation. While our analysis of brightness temperature characteristics did not show large discrepancies between simulations and observations (Hernandez-Carrascal et al., 2012), more subtle differences can not be ruled out. It may also be partly due to a bias in the CLA (cloud analysis) product used to estimate the cloud top pressure in the AMV derivation prototype. However, our tests suggest that the differences between the AMV pressure and the pressure of the cloud top are clearly smaller than the differences between the AMV pressure and the representative pressure, and that the differences between the cloud top pressure and the best fit pressure are large; the underestimation of the representative pressure in our dataset might actually be partly caused by its reasonably good estimation of the cloud top pressure.

The present study suggests that it is beneficial to assign AMVs to a representative level within the cloud, rather than to an estimate of the cloud top for high-level AMVs or to an estimate of the cloud base for low-level AMVs, as is current practice. Further work is required to determine how this representative level can be derived in the absence of the detailed cloud information that is accessible in our simulation framework. Also, the finding suggests that it may either be beneficial to use height assignments specifically designed for AMVs (rather than general cloud top pressure products), or to develop height assignment corrections that are specifically designed to account for AMV characteristics (possibly derived on the user-side). This aspect requires further discussion in the community; for practical reasons it may be best to continue to assign AMVs to the best available estimate of the cloud top, but to develop corrections to the height assignment on the user side.

The detailed description of the atmosphere provided by a simulation framework offers new opportunities to analyse AMVs. This paper has shown some examples, but many other are possible. Regarding alternative views of what AMVs may represent, there are other possibilities to explore, such as an average over a small interval below the top or a variant of *pMean* where a limit is set to the difference between the pressure of the top and the layer-average pressure. The use of a Gaussian filter instead of a boxcar filter for vertical averaging could also be explored. Further investigations are possible with the simulated dataset, for instance, to investigate the origins of the correlated errors by using alternative AMV height interpretations as used elsewhere in this study. The new opportunities provided by a simulation framework go beyond the analysis of AMVs. For instance, a potential use of simulated imagery would be to validate cloud classifications from observed imagery.

Perhaps the main conclusion of this study is that the simulation framework is a very powerful approach. It opens new avenues for progress both in AMV derivation and in data assimilation. Regarding AMV derivation, it allows to study how specific ambient conditions affect AMV statistics, and also provides useful tools for case studies and for detailed height assignment analysis. Regarding AMV data assimilation, it allows to assess alternative interpretations of the nature of AMVs, and it makes it possible to estimate spatial, vertical and temporal error correlations related to each specific observation operator. However, it is important to keep in mind that the approach has its limitations as well. There are issues related to the model simulation, concerning e.g. the resolution, the realism of cloud structures or the spin-up period. The length of the study period is also an important point: in our study it was just one day, but the amount of data from the model output was huge. There is also the issue of the methodology: this is early days for the approach, and appropriate methods need to be developed and refined. Similar studies are currently ongoing by Lean et al. (2012).

Acknowledgements

The study was funded by EUMETSAT contract EUM/CO/10/46000000785/RB. We wish to express our thanks to Régis Borde for his support during the project and for producing the AMVs for the study, to Hans-Joachim Lutz for the cloud analysis used in the AMV derivation, to Steve Wanzong and CIMSS for providing the WRF simulation output, and to Mary Forsythe and to Tony McNally for their interesting comments and questions.

References

Borde, R. and R. Oyama (2008). A direct link between feature tracking and height assignment of operational Atmospheric Motion Vectors. *Proceedings of the Ninth International Winds Workshop, Annapolis, Maryland, USA, 14-18 April 2008*.

Borde, R., A. D. Smet, G. Dew, P. Watts, H.-J. Lutz, M. Carranza, and M. Doutriaux-Boucher (2011). AMV extraction scheme for MTG-FCI at EUMETSAT. *Proceedings of the 2011 EUMETSAT Conference, Oslo, Norway, 5-9 Sep 2011*.

Bormann, N., G. Kelly, and J.-N. Thépaut (2002). Characterising and correcting speed biases in Atmospheric Motion Vectors within the ECMWF system. *Proceedings of the Sixth International Winds Workshop, Madison, Wisconsin, USA, 7-10 May 2002*.

Büche, G., H. Karbstein, A. Kummer, and H. Fischer (2006). Water Vapor Structure Displacements from Cloud-Free Meteosat Scenes and Their Interpretation for the Wind Field. *J. Appl. Meteor. Climatol. 45*, 556–575.

Cotton, J. and M. Forsythe (2010). NWP SAF AMV monitoring, 4th analysis report. The Met. Office, Exeter, United Kingdom. *Available online from: http://research.metoffice.gov.uk/research/interproj/nwpsaf/satwind_report/analysis.html*.

Forsythe, M., J. Cotton, and R. Saunders (2010). Improving AMV impact in NWP. *Proceedings of the Tenth International Winds Workshop, Tokyo, Japan, 22-26 Feb 2010*.

Hasler, A. F., W. C. Skillman, and W. E. Shenk (1979). In situ aircraft verification of the quality of satellite cloud winds over oceanic regions. *Journal Appl. Meteor. 18*, 1481–1489.

Hernandez-Carrascal, A., N. Bormann, R. Borde, H.-J. Lutz, and S. Wanzong (2012). Atmospheric Motion Vectors from model simulations. Part I: Methods and characterisation as single-level estimates of wind. *ECMWF Technical Memorandum No. 677*.

Lean, P., S. Migliorini, and G. Kelly (2012). Studying the relationship between synthetic NWP-derived AMVs and model winds. *Proceedings of the Eleventh International Winds Workshop, Auckland, New Zealand, 20-24 Feb 2012*.

Otkin, J. A., T. J. Greenwald, J. Sieglaff, and H.-L. Huang (2009). Validation of a Large-Scale Simulated Brightness Temperature Dataset Using SEVIRI Satellite Observations. *J. Appl. Meteor. Climatol. 48*, 1613–1626.

Rao, P. A., C. S. Velden, and S. A. Braun (2002). The vertical error characteristics of GOES-derived winds: Description and experiments with numerical weather prediction. *J. Appl. Meteorol. 41*, 253–271.

Rao, P. K., S. J. Holmes, R. K. Anderson, J. S. Winston, and P. E. Lehr (eds) (1990). *Weather Satellites: Systems, Data, and Environmental Applications*. Boston, USA: American Meteorological Society.

Salonen, K., J. Cotton, N. Bormann, and M. Forsythe (2012). Characterising AMV height assignment error by comparing best-fit pressure statistics from the Met Office and ECMWF system. *Proceedings of the Eleventh International Winds Workshop, Auckland, New Zealand, 20-24 Feb 2012*.

Saunders, R., M. Matricardi, P. Rayer, T. Blackmore, N. Bormann, D. Salmond, A. Geer, P. Brunel, and P. Marguinaud (2008). What can RTTOV-9 do for me? *Proceedings of the 16th international TOVS study conference, Angra dos Reis, Brazil, 7-13 May 2008*.

Skamarock, W. C., J. B. Klemp, J. Dudhia, D. O. Gill, D. M. Barker, W. Wang, and J. G. Powers (2005). A description of the Advanced Research WRF version 2. *NCAR Tech. Note TN-4681STR, 88 pp*.

Thompson, G., P. R. Field, R. M. Rasmussen, and W. Hall (2008). Explicit forecasts of winter precipitation using an improved bulk microphysics scheme. Part II: Implementation of a new snow parameterization. *Mon. Wea. Rev. 136*, 5095–5115.

Velden, C. S. and K. M. Bedka (2009). Identifying the Uncertainty in Determining Satellite-Derived Atmospheric Motion Vector Height Attribution. *J. Appl. Meteor. Climatol. 48*, 450–463.

von Bremen, L. (2008). Using simulated satellite images to improve the characterization of Atmospheric Motion Vectors (AMVs) and their errors for Numerical Weather Prediction. *NWP SAF report NWPSAF-EC-VS-015. Available from http://research.metoffice.gov.uk/research/interproj/nwpsaf/vs.html*.

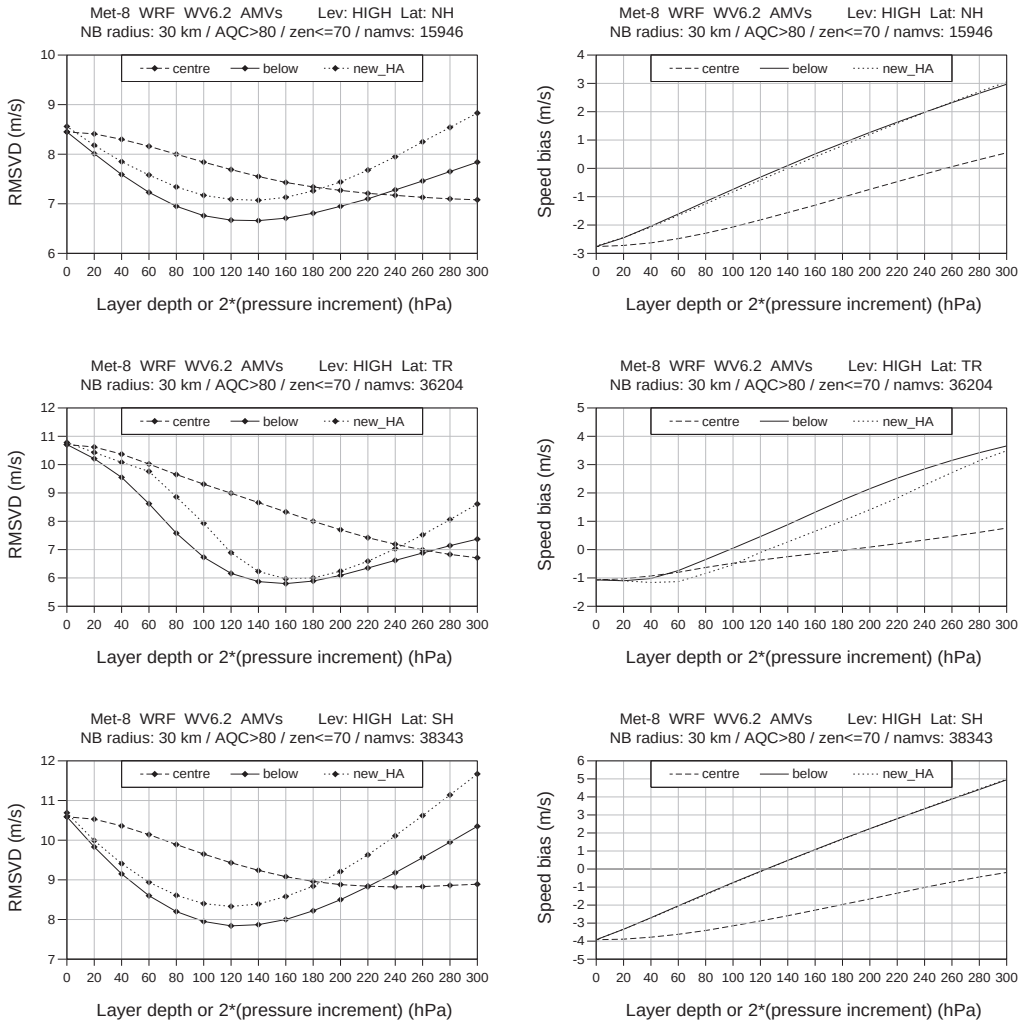

Figure 1: RMSVD (left) and bias curves (right), as layer depth (or pressure increment) increases, for high-level AMVs from WRF WV6.2 imagery for the northern hemisphere extra-tropics (top), tropics (middle) and the southern hemisphere extra-tropics (bottom). Each panel shows curves for AMVs interpreted as vertical averages over a layer centred around the original pressure (dashed), as vertical averages over a layer just below the original level (solid), and evaluated after being assigned to an increased pressure (dotted). Notice that in the last case the x-axis shows two times the pressure increment, while for the other curves it shows the layer depth. In the cases of layer averaging, the model winds were also averaged horizontally over a 30 km neighbourhood. Only winds with a model independent QI $> 80\%$ *have been selected.*

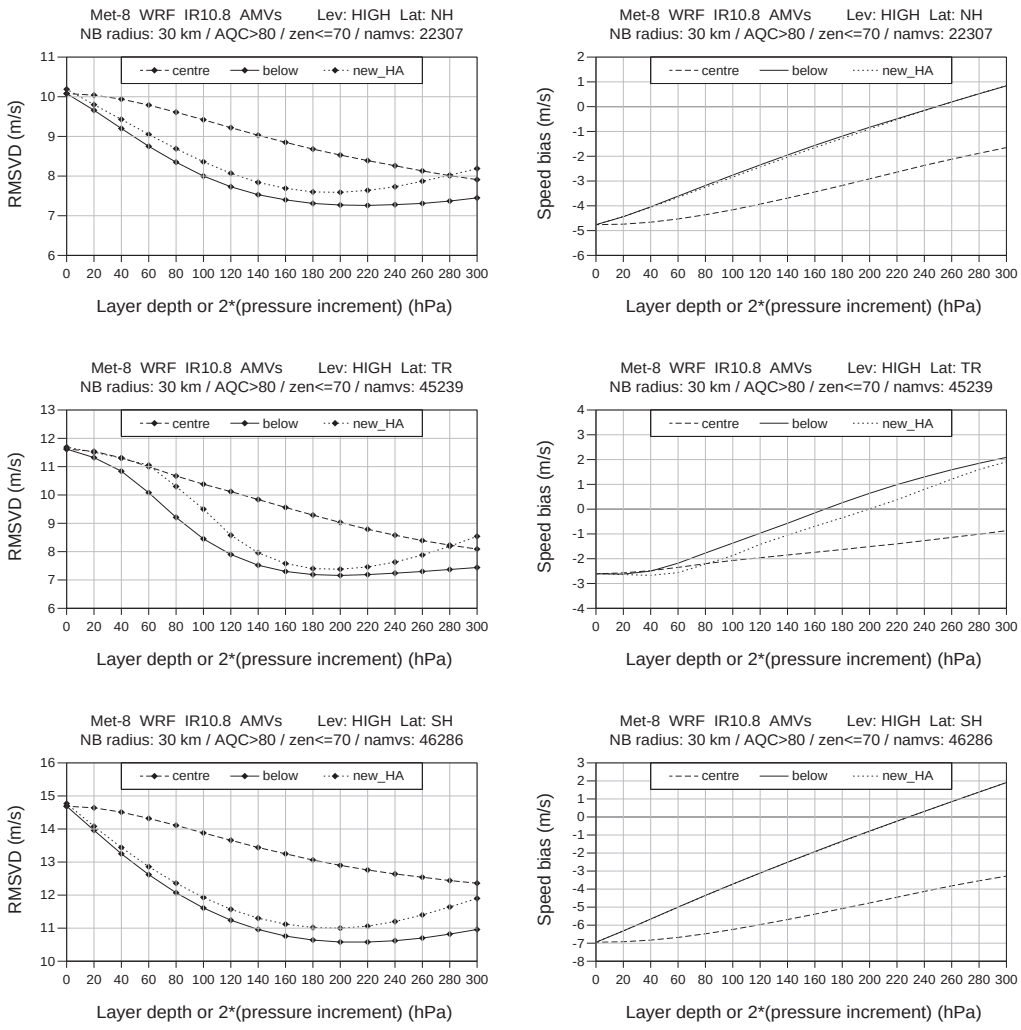

Figure 2: As Fig. 1, for high level AMVs derived from the WRF IR10.8 imagery.

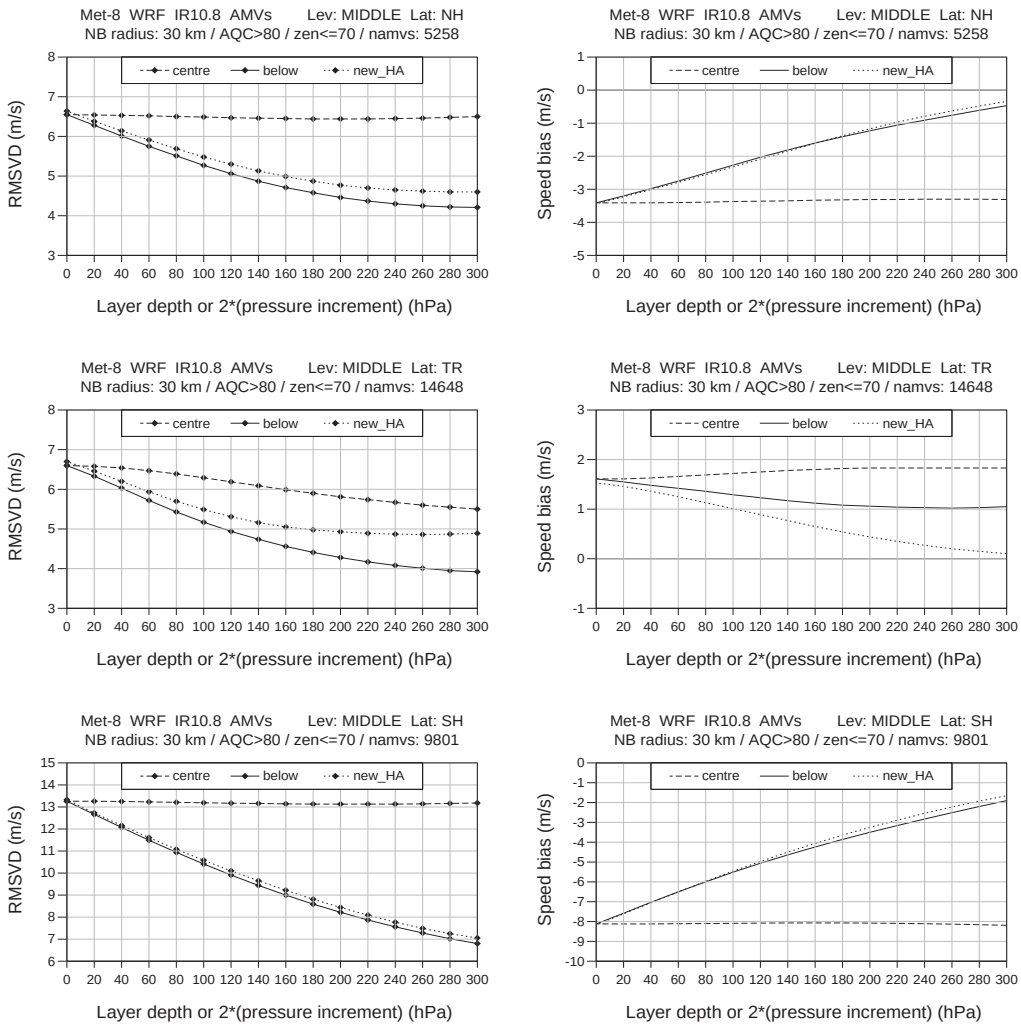

Figure 3: As in Figure 1, for middle-level AMVs from the WRF IR10.8 imagery.

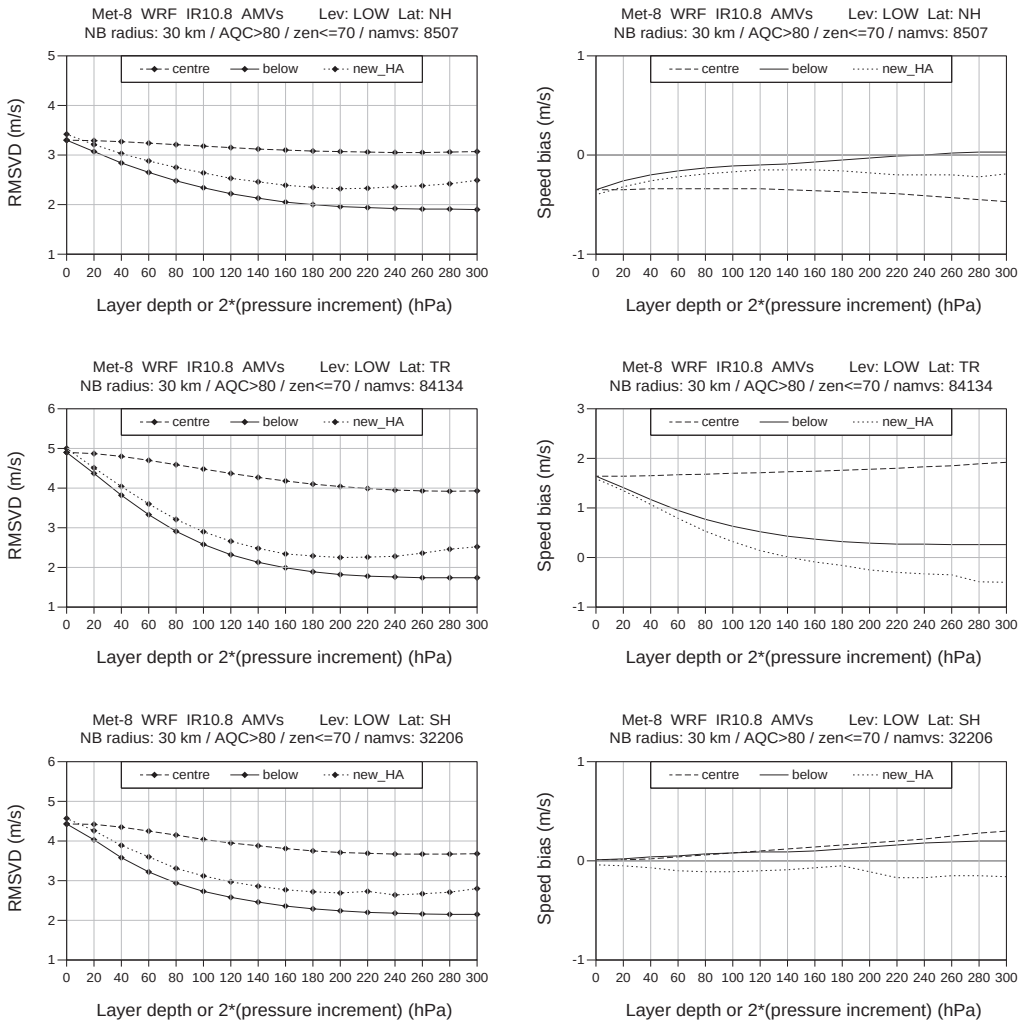

Figure 4: As in Figure 1, for low-level AMVs from the WRF IR10.8 imagery. Note that for the new_HA *curve, AMVs located below the lowest model level after the height reassignment were omitted (roughly half the number of AMVs at the largest reassignment shown), whereas for the other curves all winds were included, but the layer was restricted as described in the main text.*

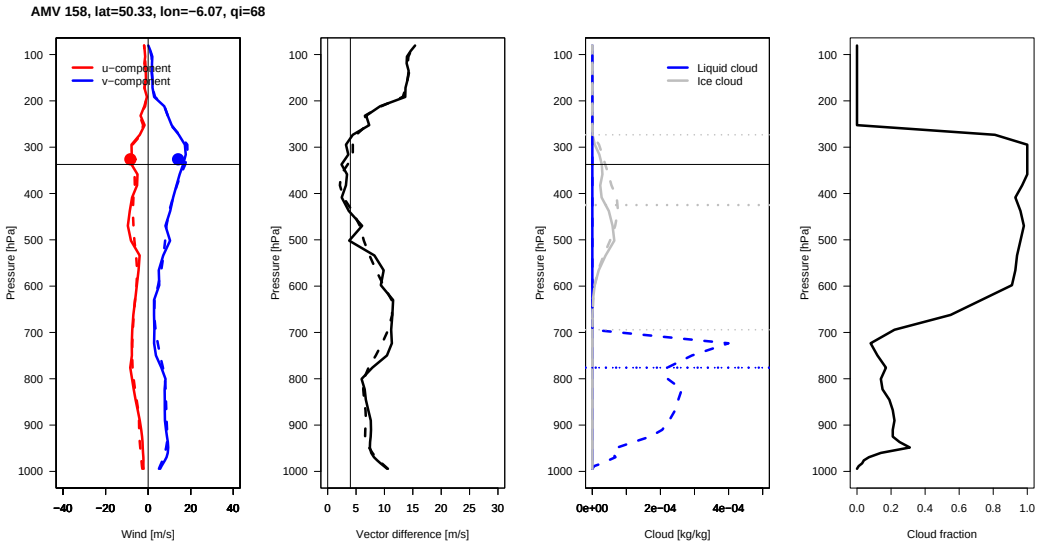

Figure 5: Example of model profiles collocated with an AMV. The first panel shows the model u and v profiles (lines) and u and v from the AMV (dots), the second panel shows the profile of vector differences between the AMV and the model wind profile, the third panel shows the profiles of ice and liquid-water mixing ratios, and the fourth panel shows the cloud fraction. For the wind and the mixing ratio panels, solid lines show profiles at the grid-point nearest to the AMV location, whereas dashed lines show average values in a 30 km neighbourhood. Also shown are the level of best fit (black horizontal line) and the top and bottom of the diagnosed cloud layers (dotted lines in the mixing ratio panel).

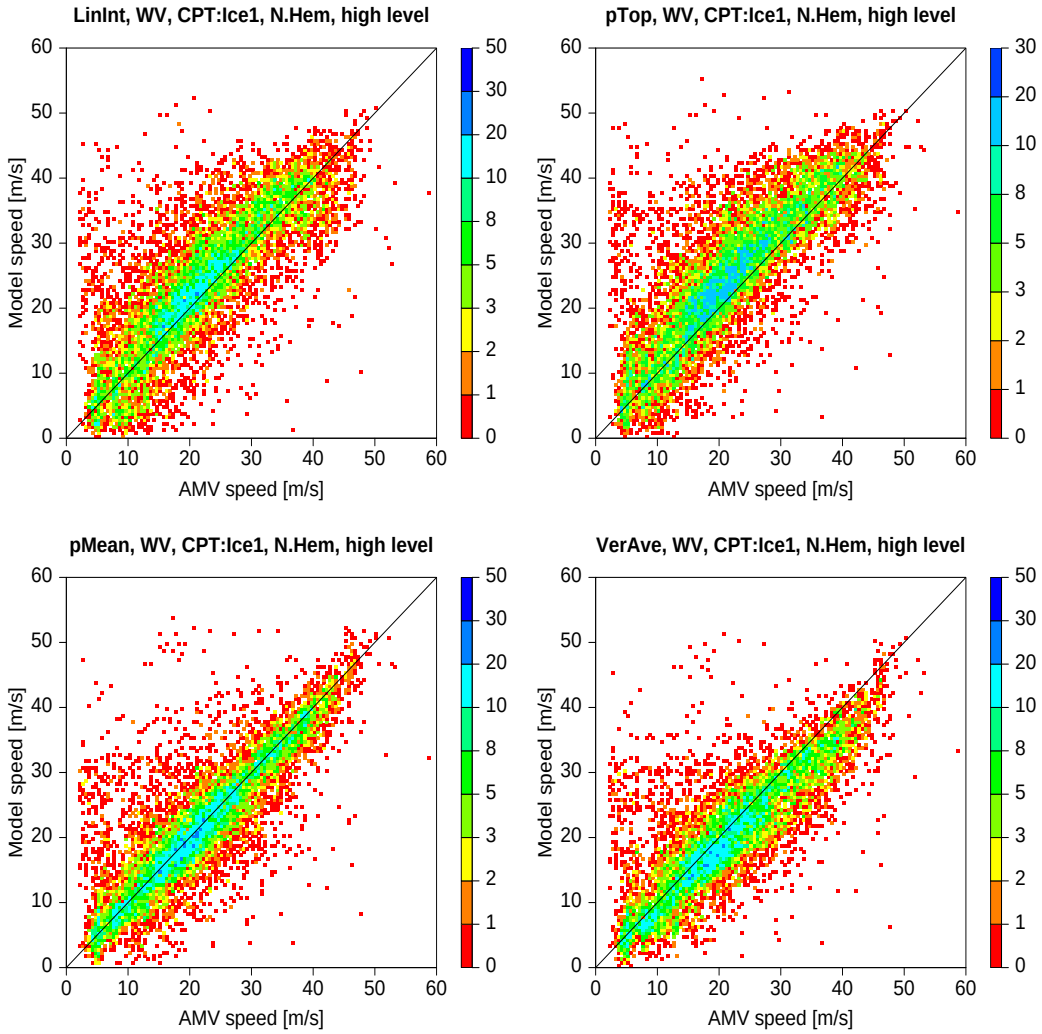

Figure 6: 2D histograms of speed for high-level AMVs derived from the WRF WV6.2 simulated images for northern hemisphere extra-tropics, for the model wind calculated by linear interpolation of the wind profile to the original AMV pressure (top left), to the pressure of the top of the layer (top right), to a layer-average pressure (bottom left), and for the model wind calculated as an average of wind over the cloud layer (bottom right). Only AMVs with an Ice1 profile and a model-independent QI > 80% have been selected.

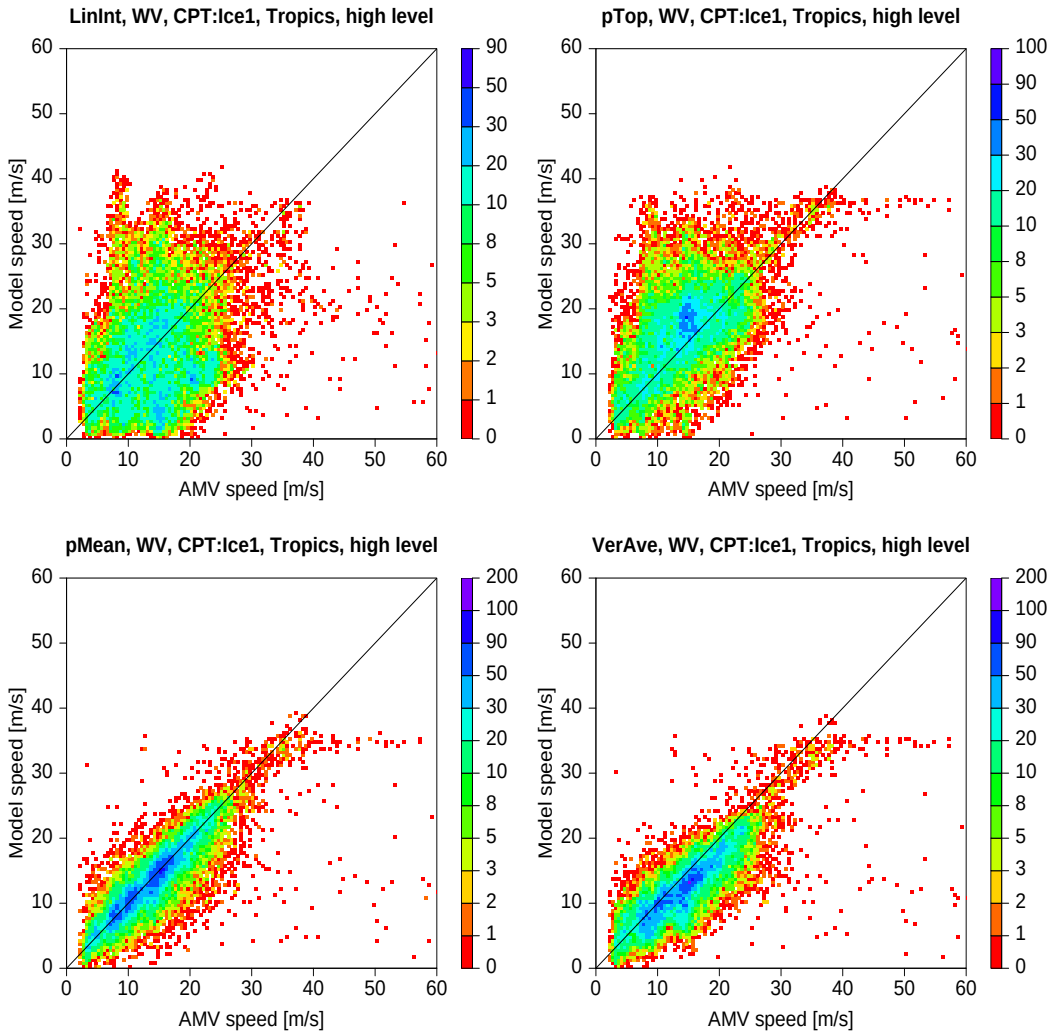

Figure 7: As Fig. 6, for tropics.

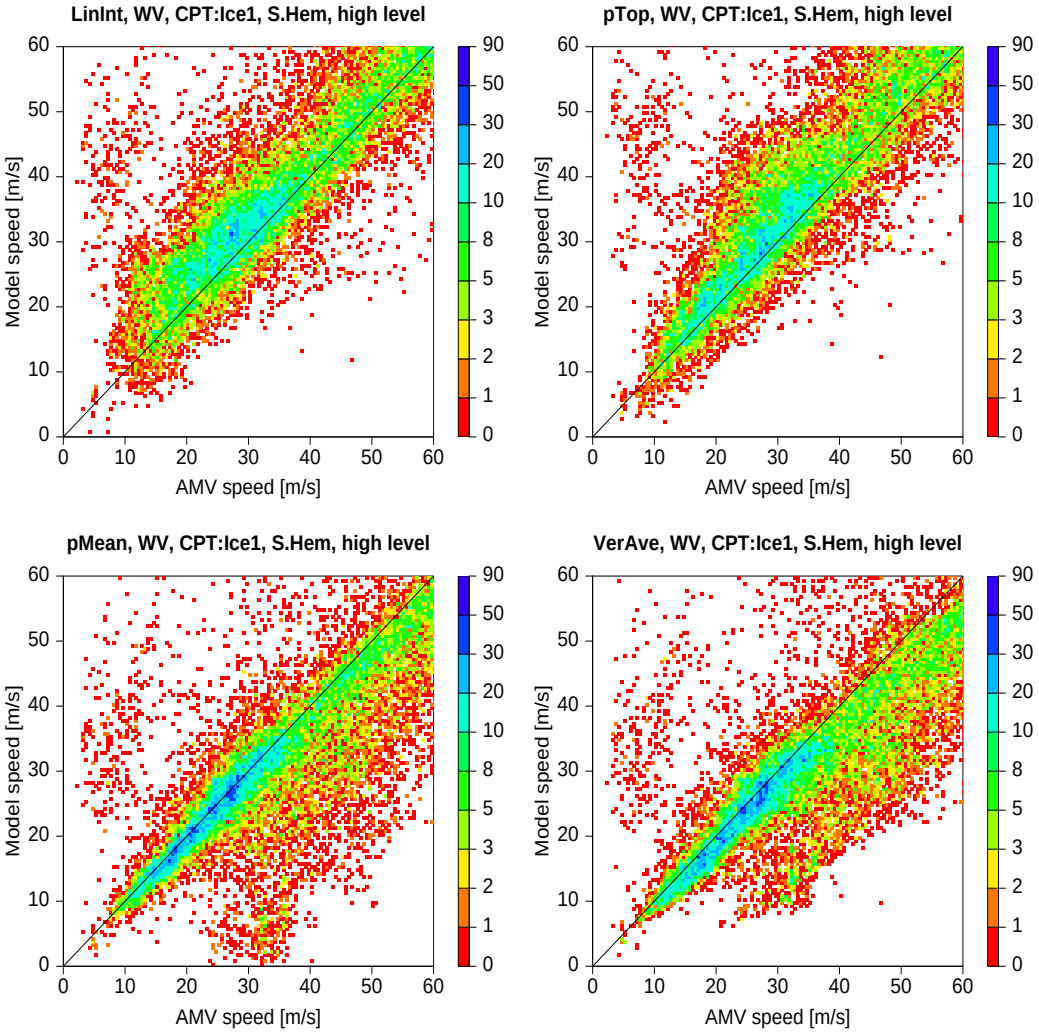

Figure 8: As Fig. 6, for southern hemisphere extra-tropics.

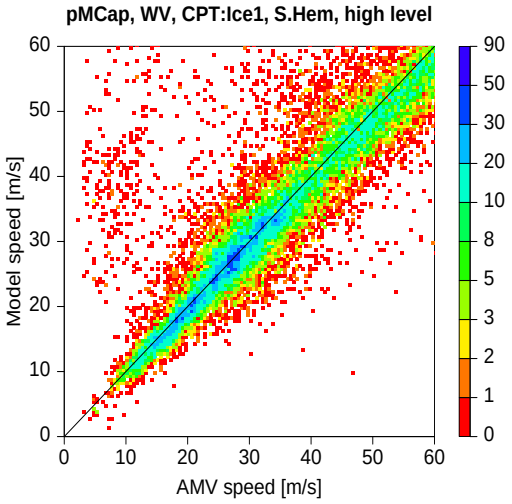

Figure 9: As Fig. 8, for pMCap, a variant of pMean, for cap = 100 hPa (details in main text).

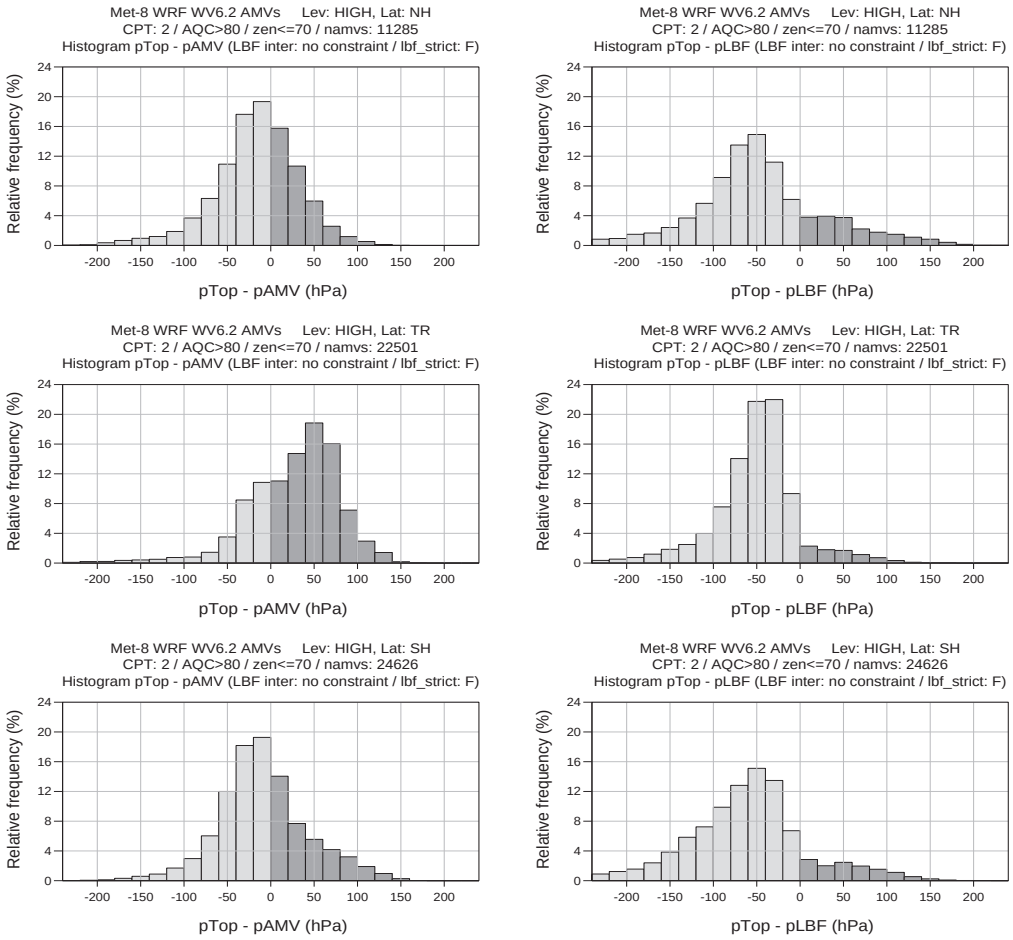

Figure 10: Left column: histograms of pTop (model cloud top pressure) - pAMV (pressure assigned during the derivation) for AMVs derived from the WRF WV6.2 simulated images, for northern hemisphere extra-tropics (top), tropics (middle) and southern hemisphere extra-tropics (bottom). Right column: as left column, but for pTop - pLBF (pressure of the level of best fit). Only AMVs classified as Ice1 have been taken into account.

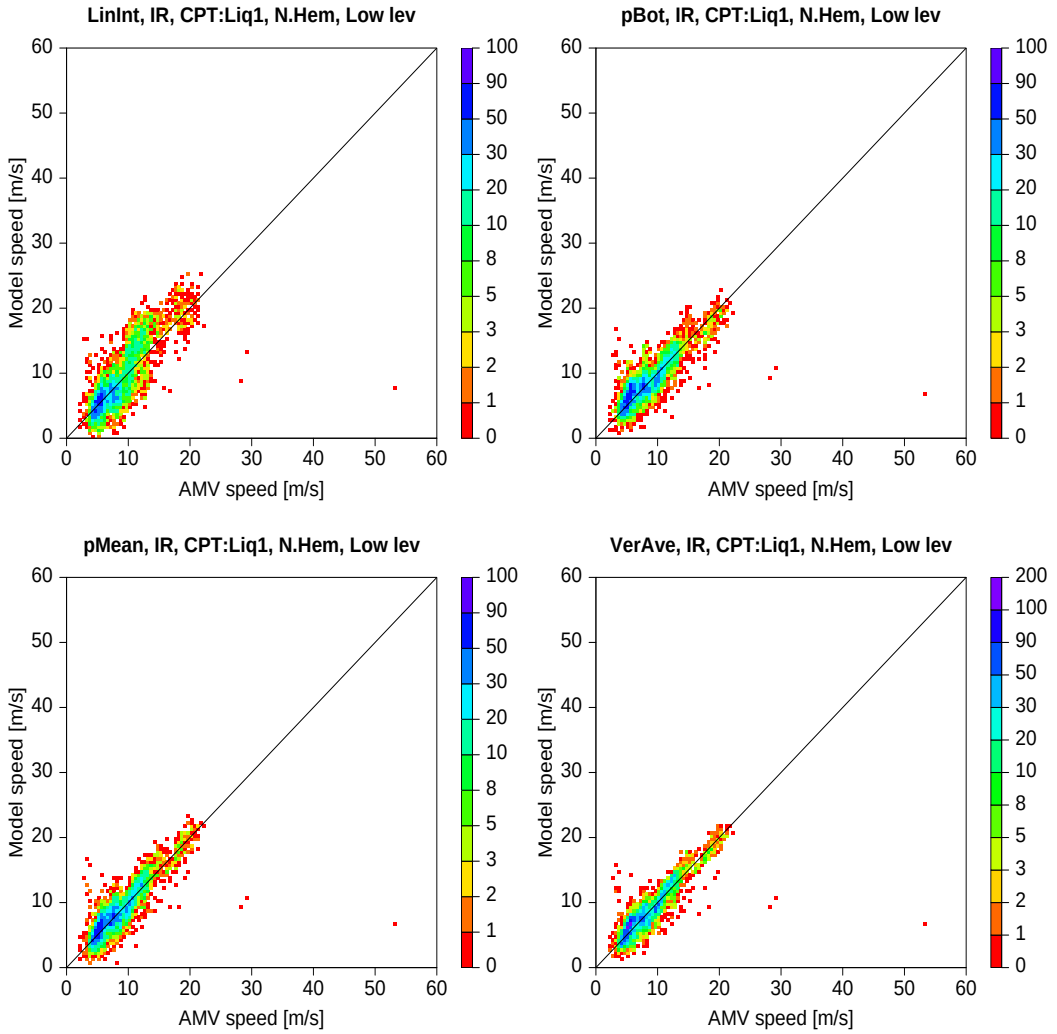

Figure 11: 2D histograms of speed for low-level AMVs derived from the WRF IR10.8 simulated images for northern hemisphere extra-tropics, for the model wind calculated by linear interpolation of the wind profile to the original AMV pressure (top left), to the pressure of the bottom of the layer (top right), to a layer-average pressure (bottom left), and for model wind calculated as an average of wind over the cloud layer (bottom right). Only AMVs with a Liq1 profile and a model-independent QI $>$ *80% have been selected.*

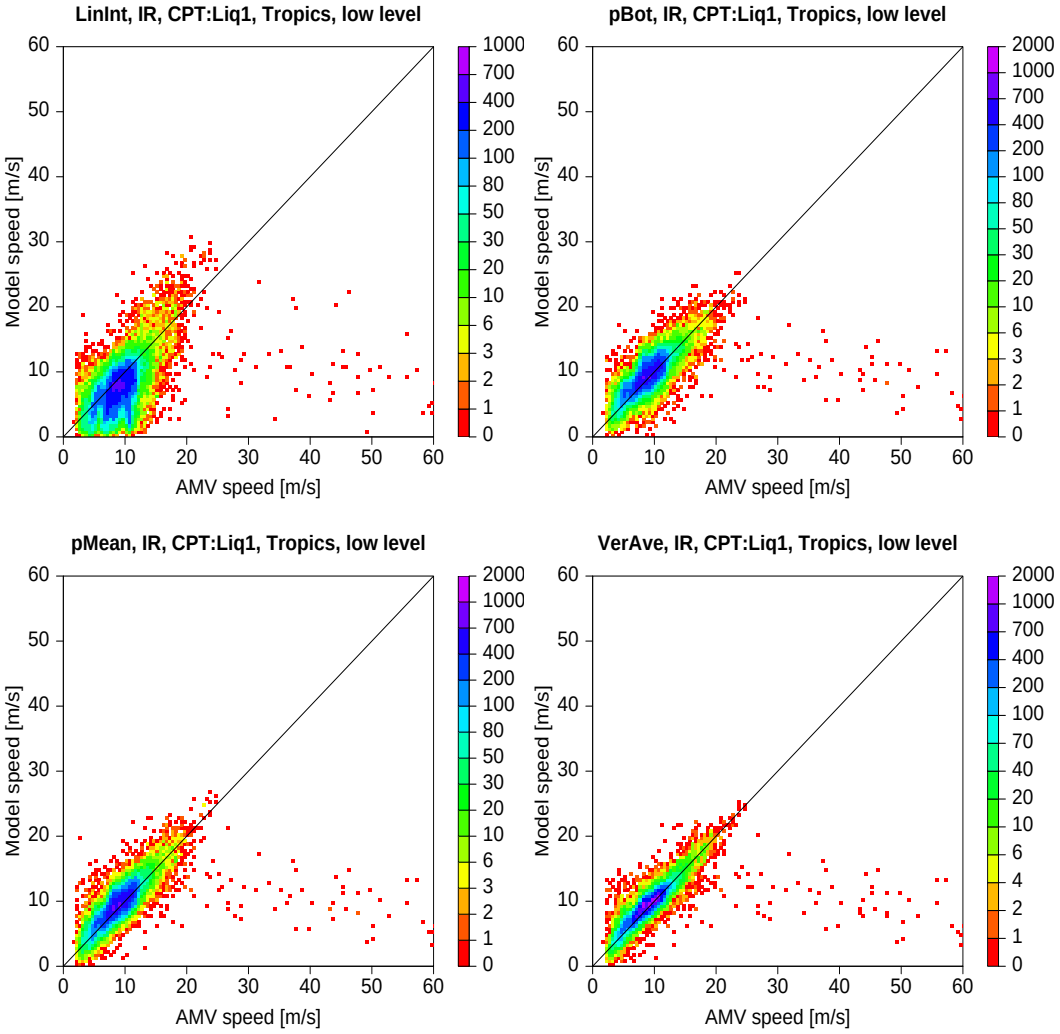

Figure 12: As Fig. 11, for tropics.

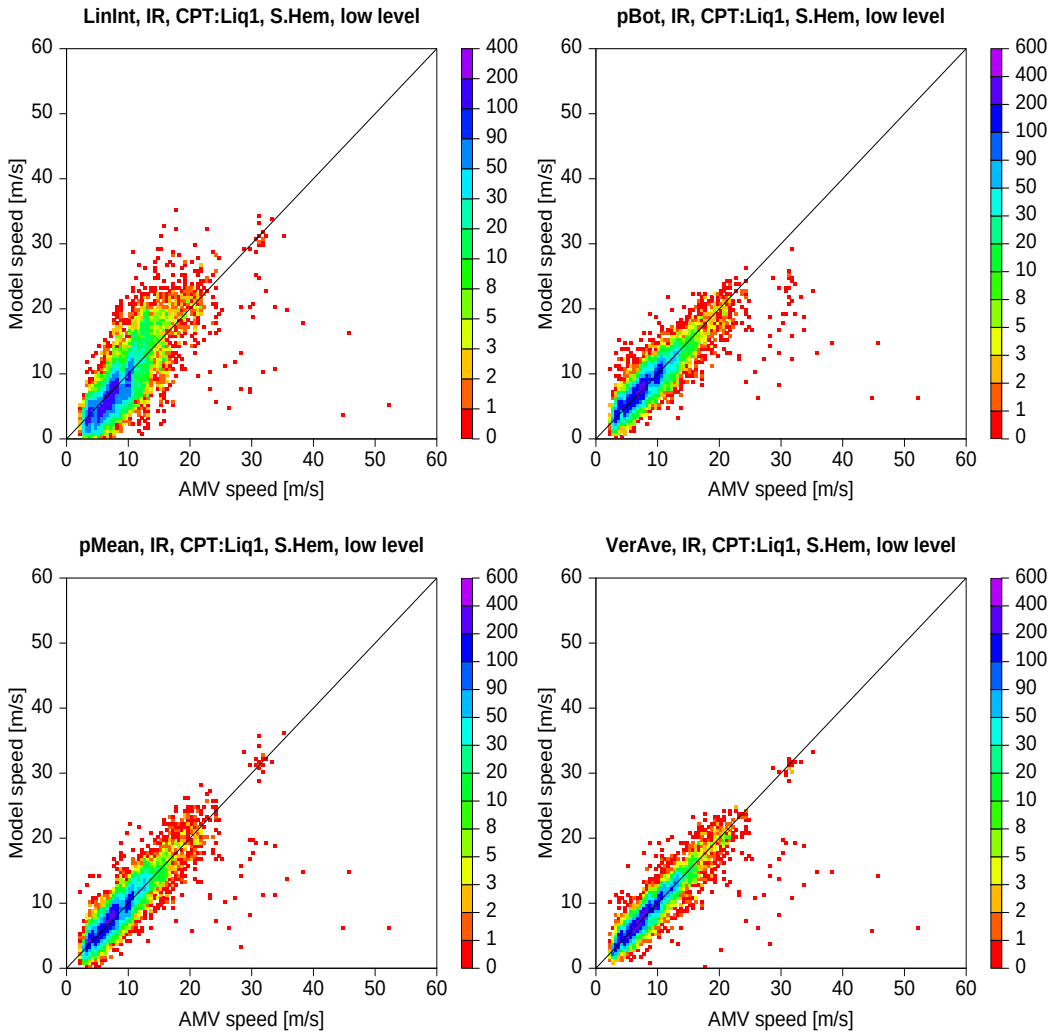

Figure 13: As Fig. 11, for southern hemisphere extra-tropics.

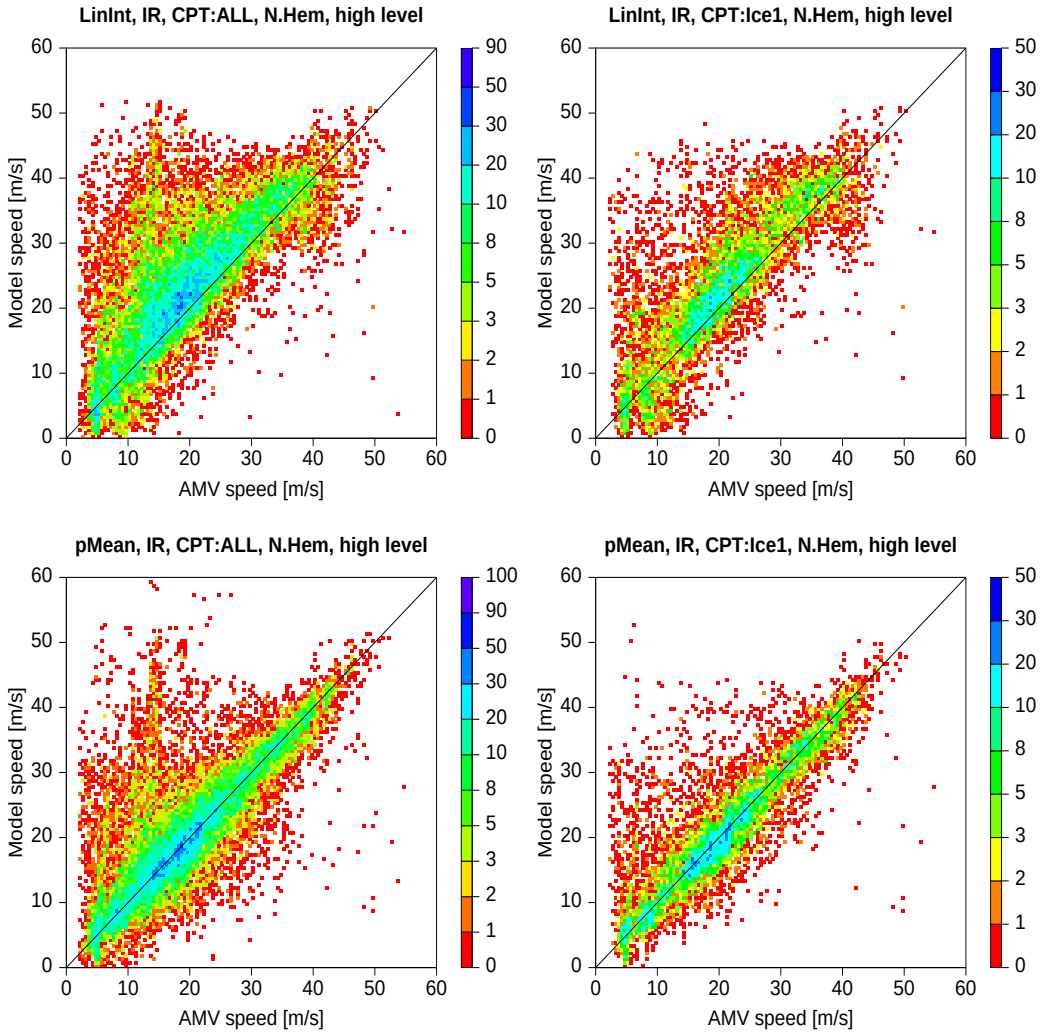

Figure 14: 2D histograms of speed for high-level AMVs derived from the WRF IR10.8 images, with a model-independent QI > 80%, for model wind calculated by linear interpolation to the assigned AMV pressure (LinInt, top), and by linear interpolation to a pressure averaged over the top cloud layer (pMean, bottom). The left column shows all AMVs regardless of the cloud profile type, and the right column shows the subset of AMVs with a cloud profile type Ice1 (i.e. with one layer of ice cloud).

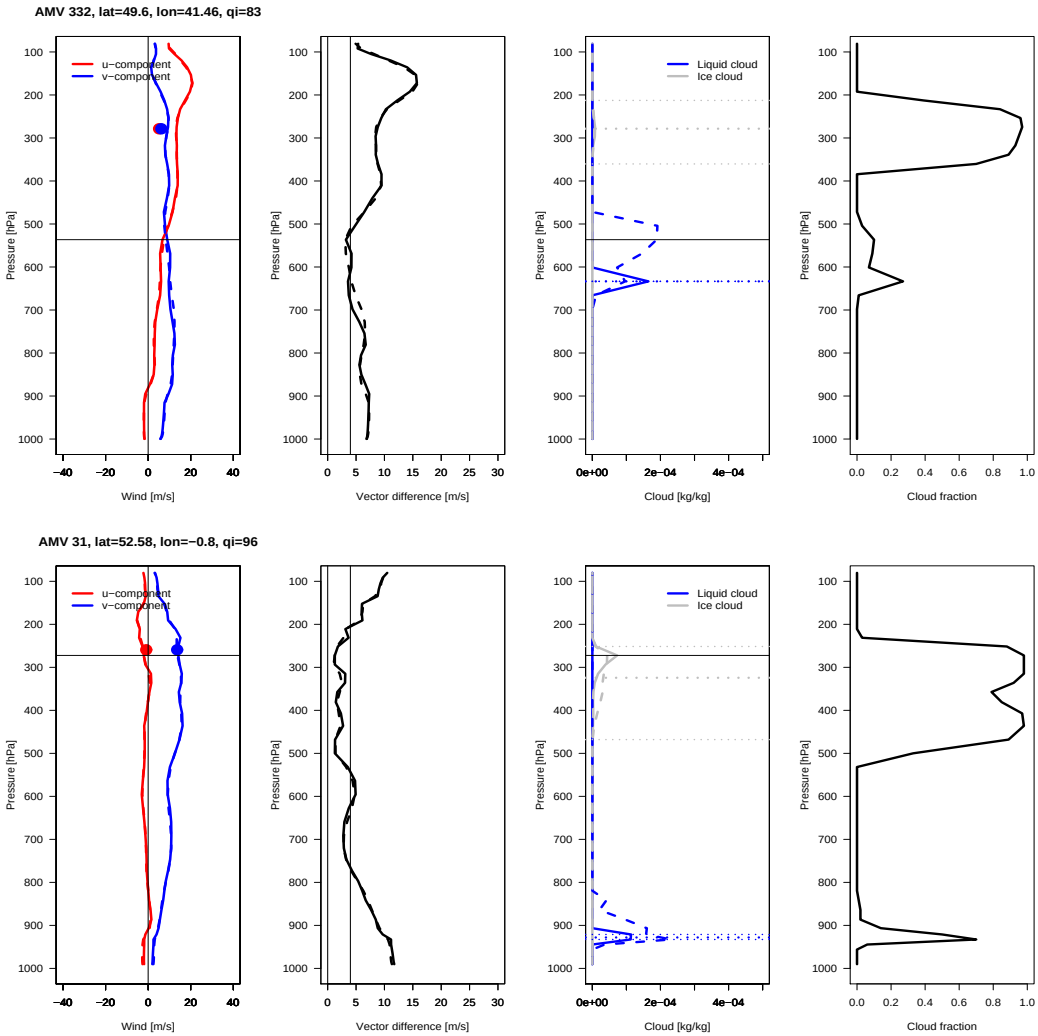

Figure 15: As Figure 5, but for two examples of high-level WRF IR10.8 AMVs with one ice cloud and one liquid water cloud layer.

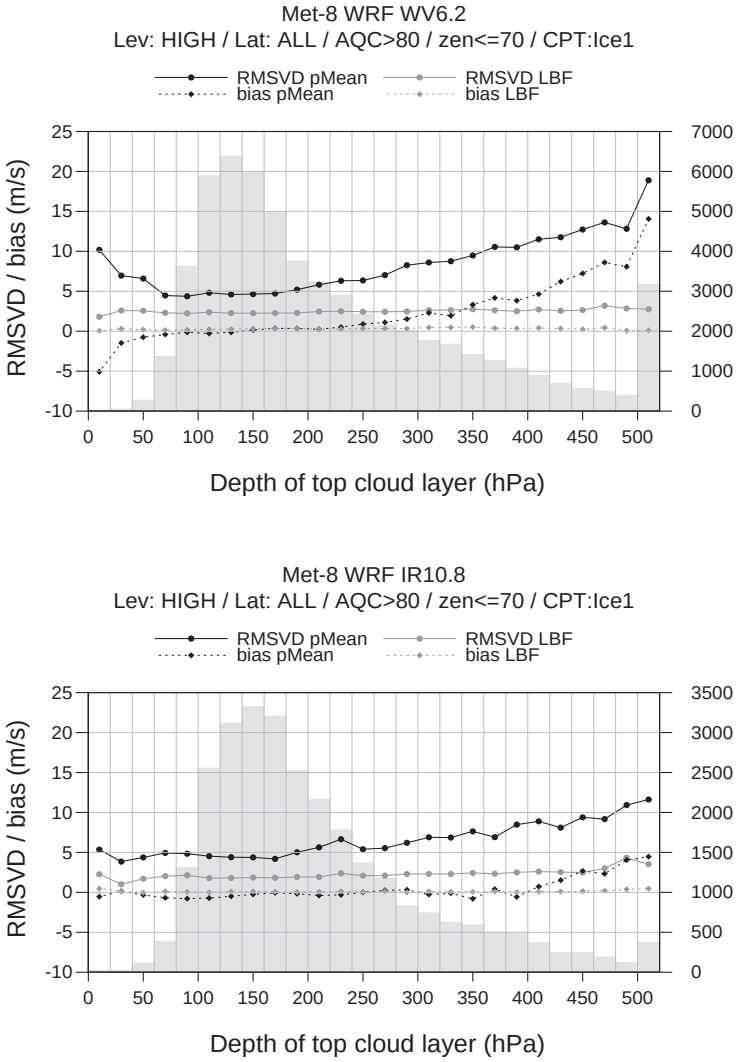

Figure 16: RMSVD and bias curves for high-level AMVs from the WRF WV6.2 images (top) and IR10.8 (bottom) for AMVs interpreted as single-level point estimate of winds reassigned to a layer-average pressure. Statistics for the LBF pressure are also included, for reference. The scale on the right y-axis represents the number of AMVs in each bin.

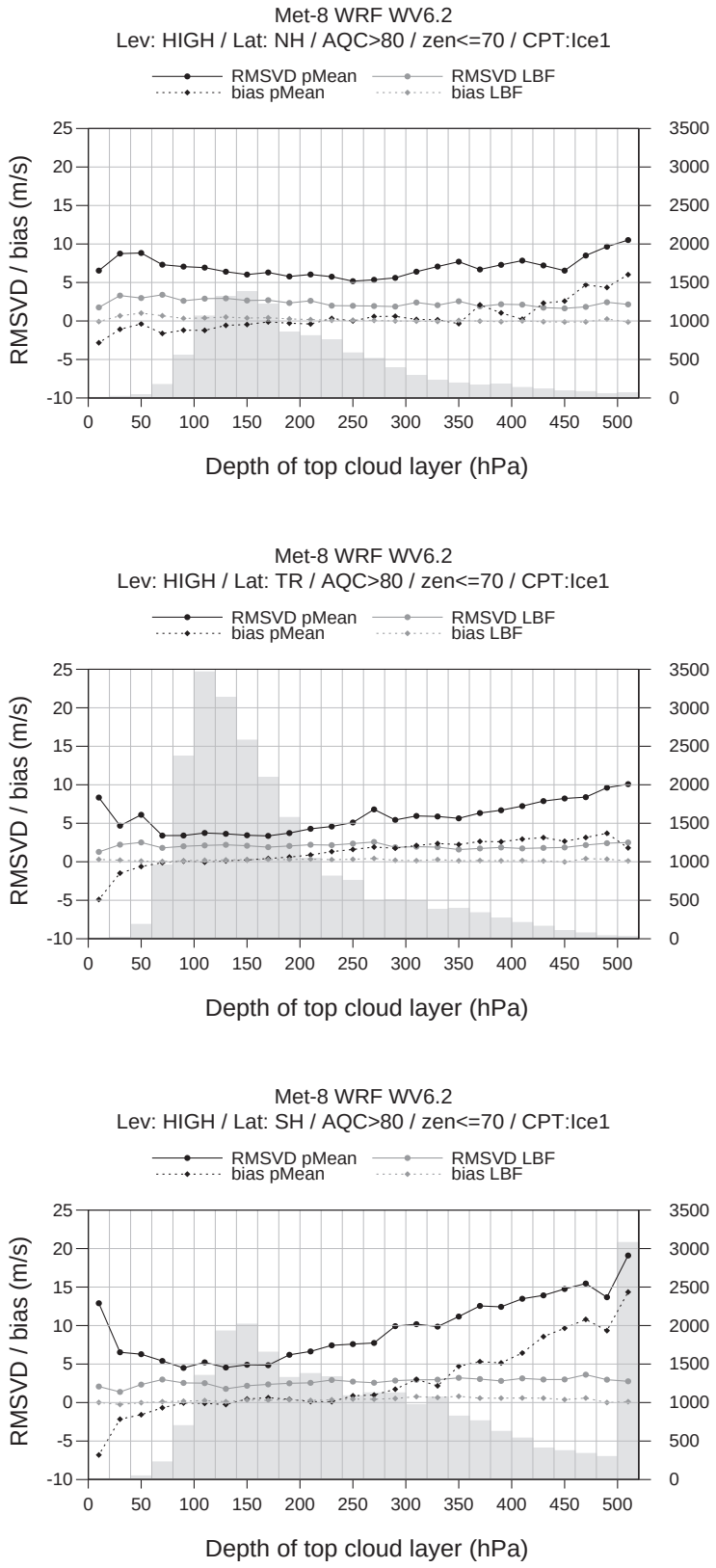

Figure 17: As in Fig. 16, for high-level WRF WV6.2 AMVs, for northern hemisphere extra-tropics (top), tropics (middle) and southern hemisphere extra-tropics (bottom).